

## APOGEE [C/N] ABUNDANCES ACROSS THE GALAXY: MIGRATION AND INFALL FROM RED GIANT AGES

STEN HASSELQUIST<sup>1</sup>, JON A. HOLTZMAN<sup>1</sup>, MATTHEW SHETRONE<sup>2</sup>, JAMIE TAYAR<sup>3</sup>, DAVID H. WEINBERG<sup>3</sup>, DIANE FEUILLET<sup>5</sup>, KATIA CUNHA<sup>6</sup>, MARC H. PINSONNEAULT<sup>3</sup>, JENNIFER A. JOHNSON<sup>3</sup>, JONATHAN BIRD<sup>4</sup>, TIMOTHY C. BEERS<sup>7</sup>, RICARDO SCHIAVON<sup>14</sup>, IVAN MINCHEV<sup>13</sup>, J. G. FERNÁNDEZ-TRINCADO<sup>8,9,10</sup>, D. A. GARCÍA-HERNÁNDEZ<sup>11,12</sup>, CHRISTIAN NITSCHHELM<sup>15</sup>, OLGA ZAMORA<sup>11,12</sup>

*Draft version December 13, 2018*

### ABSTRACT

We present [C/N]-[Fe/H] abundance trends from the SDSS-IV Apache Point Observatory Galactic Evolution Experiment (APOGEE) survey, Data Release 14 (DR14), for red giant branch stars across the Milky Way Galaxy (MW,  $3 \text{ kpc} < R < 15 \text{ kpc}$ ). The carbon-to-nitrogen ratio (often expressed as [C/N]) can indicate the mass of a red giant star, from which an age can be inferred. Using masses and ages derived by Martig et al., we demonstrate that we are able to interpret the DR14 [C/N]-[Fe/H] abundance distributions as trends in age-[Fe/H] space. Our results show that an anti-correlation between age and metallicity, which is predicted by simple chemical evolution models, is not present at any Galactic zone. Stars far from the plane ( $|Z| > 1 \text{ kpc}$ ) exhibit a radial gradient in [C/N] ( $\sim -0.04 \text{ dex/kpc}$ ). The [C/N] dispersion increases toward the plane ( $\sigma_{[C/N]} = 0.13$  at  $|Z| > 1 \text{ kpc}$  to  $\sigma_{[C/N]} = 0.18 \text{ dex}$  at  $|Z| < 0.5 \text{ kpc}$ ). We measure a disk metallicity gradient for the youngest stars (age  $< 2.5 \text{ Gyr}$ ) of  $-0.060 \text{ dex/kpc}$  from 6 kpc to 12 kpc, which is in agreement with the gradient found using young CoRoGEE stars by Anders et al. Older stars exhibit a flatter gradient ( $-0.016 \text{ dex/kpc}$ ), which is predicted by simulations in which stars migrate from their birth radii. We also find that radial migration is a plausible explanation for the observed upturn of the [C/N]-[Fe/H] abundance trends in the outer Galaxy, where the metal-rich stars are relatively enhanced in [C/N].

*Keywords:* Galaxy: disk, Galaxy: abundances

### 1. INTRODUCTION

The SDSS-IV Apache Point Observatory Galactic Evolution Experiment (APOGEE, [Majewski et al. 2017](#)) survey provides detailed chemical abundances of 18 chemical elements for  $\sim 10^5$  red giant stars across the disk of the Milky Way (MW) Galaxy (3-15 kpc). From this extensive data set, maps

of the chemical abundance distributions of the disk can be generated. Valuable information about the chemical evolution and star-formation history of the MW disk can be inferred from these maps, as done in the APOGEE “chemical cartography” program (see [Hayden et al. 2014, 2015](#); [J. Holtzman et al.](#), in prep.). However, unlike most chemical abundances provided by APOGEE, the abundances of carbon and nitrogen in red giant stars are not necessarily a reflection of the stellar primordial abundance as the observed ratio of these elements can be altered due to stellar evolution, thus complicating the interpretation of C and N abundance maps across the Galaxy.

It has been shown that the atmospheric C-to-N abundance ratio that a star is formed with (often expressed as [C/N]) changes as a star evolves from the main sequence to the red giant branch (see, e.g., [Iben 1965](#); [Salaris et al. 2015](#)). As the star ascends the giant branch, the convective layer extends towards the core where CN-cycle processed material lies. This material is enhanced in N relative to the star’s outer layers. The depth of this layer, and therefore how much nitrogen-enhanced material is dredged up, depends on the mass of the star. Consequently, the observed [C/N] abundance for a star on the giant branch can indicate the *mass* of the star, from which an *age* can be inferred by invoking models for stellar evolution.

This phenomenon has been exploited in the APOGEE sample to show that the  $\alpha$ -element enhanced stars in the MW disk are generally older than the disk stars with Solar  $\alpha$ -element abundance ([Masseron & Gilmore 2015](#)), although there exist a few  $\alpha$ -element enhanced young stars in the Solar Neighborhood (see, e.g., [Chiappini et al. 2015](#) and [Martig et al. 2015](#)). Additionally, [Martig et al. \(2016b\)](#) and [Ness et al. \(2016\)](#) have derived ages for the APOGEE DR12 sample using masses from asteroseismology, showing that there is an age gradient in the geometrically-defined thick disk ([Martig et al. 2016a](#)), indicating that this structure is not uniformly old across all

<sup>1</sup> New Mexico State University, Las Cruces, NM 88003, USA (sten@nmsu.edu, holtz@nmsu.edu)

<sup>2</sup> University of Texas at Austin, McDonald Observatory, Fort Davis, TX 79734, USA (shetrone@utexas.edu)

<sup>3</sup> Department of Astronomy, The Ohio State University, Columbus, OH 43210, USA (tayar@astronomy.ohio-state.edu, pinsonneault.1@osu.edu, johnson.3064@osu.edu, dhw@astronomy.ohio-state.edu)

<sup>4</sup> Department of Physics and Astronomy, Vanderbilt University, Nashville, TN 37235, USA (jonathan.bird@vanderbilt.edu)

<sup>5</sup> Max-Planck-Institut für Astronomie, Königstuhl 17, D-69117 Heidelberg, Germany (feuilddk@gmail.com)

<sup>6</sup> Observatório Nacional/MCTI, Rua Gen. José Cristino, 77, 20921-400, Rio de Janeiro, Brazil (cunha@email.noao.edu)

<sup>7</sup> Department of Physics and JINA Center for the Evolution of the Elements, University of Notre Dame, Notre Dame, IN 46556, USA (tbeers@nd.edu)

<sup>8</sup> Departamento de Astronomía, Casilla 160-C, Universidad de Concepción, Concepción, Chile (jfernandez@astro-udec.cl)

<sup>9</sup> Instituto de Astronomía y Ciencias Planetarias, Universidad de Atacama, Copayapu 485, Copiapó, Chile.

<sup>10</sup> Institut Utinam, CNRS UMR 6213, Université Bourgogne-Franche-Comté, OSU THETA Franche-Comté, Observatoire de Besançon, BP 1615, 25010 Besançon Cedex, France.

<sup>11</sup> Instituto de Astrofísica de Canarias, E-38205 La Laguna, Tenerife, Spain (agarcia@iac.es)

<sup>12</sup> Departamento de Astrofísica, Universidad de La Laguna (ULL), E-38206 La Laguna, Tenerife, Spain (agarcia@iac.es)

<sup>13</sup> Leibniz-Institut für Astrophysik Potsdam (AIP), An der Sternwarte 16, D-14482, Potsdam, Germany (imincev1@gmail.com)

<sup>14</sup> Astrophysics Research Institute, Liverpool John Moores University, 146 Brownlow Hill, Liverpool L3 5RF, UK (rpschiavon@gmail.com)

<sup>15</sup> Centro de Astronomía (CITEVA), Universidad de Antofagasta, Avenida Angamos 601, Antofagasta 1270300, Chile (christian.nitschhelm@uantof.cl)

Galactocentric radii.

The prospect of [C/N] abundance as an age indicator opens the possibility for studying [C/N]-metallicity or age-metallicity abundance trends across the MW disk. Simple, closed-box and leaky-box chemical evolution models suggest that the Galactic interstellar medium (ISM) should become more enriched in metals over time as stars/supernovae synthesize metals and expel some fraction of them back to the ISM. This implies that stars born at more recent times from this enriched material should be more metal-rich than stars born at older times. These simple models predict that there should be a correlation between age and metallicity for stars in the MW.

Initially, an age-metallicity relation in the Solar Neighborhood was found through Strömgren photometry of F stars (see, e.g., Twarog 1980; Carlberg et al. 1985). However, a multitude of chemical abundance studies of sub-giants in the Solar Neighborhood have shown that there is a lack of an age-metallicity relation, with large scatter in age at any given metallicity (see, e.g., Edvardsson et al. 1993; Bensby et al. 2004; Haywood et al. 2013; Feuillet et al. 2016). Simulations suggest that an age-metallicity relation can be “smeared” out by radial mixing (see, e.g., Minchev et al. 2013). Such mixing could be responsible for the metal-rich stars in the Solar Neighborhood that may be older than the more metal-poor stars (see, e.g., Fuhrmann 2008). In fact, it may be the case that large fractions of stars in the Solar Neighborhood actually migrated in from a different birth location (Chiappini et al. 2014). Feuillet et al. (2018) find that the mean age of Solar Neighborhood stars is youngest near solar metallicity and increases for both sub-solar and super-solar populations.

Radial migration, which changes a star’s orbital radius without strongly affecting its eccentricity, could occur through a variety of dynamical mechanisms. Most notably Sellwood & Binney (2002) showed that spiral arm transients could cause a star to change its guiding center radius while remaining on a near circular orbit, and they argued that this radial-mixing mechanism should operate generically in disk galaxies. In their chemical evolution models with radial mixing, Schönrich & Binney (2009a) distinguish between “blurring,” overlap of stars in radial zones because of orbital eccentricity, and “churning” that changes guiding center radii.  $N$ -body simulations show that churning is an important phenomenon in dynamically realistic disks, though the degree of mixing depends on details such as gas richness, bar formation, and satellite perturbations (e.g., Roškar et al. 2008; Bird et al. 2013; Minchev et al. 2013). It has also been suggested that radial migration could play a key role in thick-disk formation (e.g., Schönrich & Binney 2009b; Loebman et al. 2011). However, Minchev et al. (2013) find it more likely that heating by mergers is responsible for the observed properties of the inner thick disk, which consists of stars born hot in a turbulent gas-rich phase at early times (see also Minchev et al. 2017, 2018).

Two major observational constraints on the extent to which radial migration affected the spatial distributions of the MW stellar populations are the radial variation of the observed metallicity distribution functions (MDFs) and the radial variation of age-metallicity relations. Hayden et al. (2015) invoked a simple radial-migration model to explain the observed MDFs of stars observed by APOGEE across the MW. They found that such a model could explain the negatively-skewed MDF in the inner Galaxy and the positively-skewed MDF for the outer Galaxy. Loebman et al. (2016) were able

to match the change in skewness of the APOGEE MDFs with their high-resolution,  $N$ -body+smooth particle hydrodynamics (SPH) simulation by including a prescription for radial migration.

While attempts have been made to match the observed age-metallicity relation (or lack thereof) of the Solar Neighborhood using simulations with radial migration, there are few observational constraints on the age-metallicity relations across other regions of the Galaxy. Some simulations predict that there should be an increase in the relative number of outward migrators with Galactic radius, which leads to a flattening of the expected age-metallicity anti-correlation with increasing Galactic radius (e.g., Minchev et al. 2014). As large spectroscopic surveys continue to provide precise chemical abundances for stars across the Galaxy, attempts can be made to quantify radial migration in the MW, which has important implications for understanding galaxy evolution and the observed lack of age-metallicity relations (e.g., Anders et al. 2018; Minchev et al. 2018).

In this paper we present [C/N]-[Fe/H] abundance results from the latest APOGEE data release (DR14) for stars distributed across the MW disk ( $3 \text{ kpc} < R < 15 \text{ kpc}$ ). Similar to previous work, we use the [C/N] abundance of a red giant star as an indicator of its age. This work marks the first time [C/N]-[Fe/H] abundance trends of the MW have been presented in this way (individual stars rather than mean abundance/age maps), allowing for an exploration of age-metallicity relations across much of the Galaxy. From these spatially resolved age-metallicity relations, we are able to characterize the near-present day metallicity of the ISM across the Galaxy, as well as analyze how radial migration played a role in shaping these age-metallicity relations. We present and interpret [C/N]-[Fe/H] abundance trends rather than converting to age-metallicity space to avoid introducing systematic uncertainties through a [C/N]-age fit. This also allows us to explore other potential interpretations of [C/N] abundance variations across the Galaxy, which would be masked in a study that converts [C/N] to age.

The observations are described in §2. Sample selection and relating the DR14 [C/N] abundance values to mass/age are discussed in §3. We present the [C/N] abundance results in §4 and interpret them in the context of stellar age and Galactic evolution in §5.

## 2. OBSERVATIONS, DATA REDUCTION, AND ANALYSIS

The APOGEE survey was part of Sloan Digital Sky Survey III (Eisenstein et al. 2011), and observed 146,000 stars in the Milky Way galaxy (Majewski et al. 2017) from 2011-2014. APOGEE-2 began observations in 2014 as part of the Sloan Digital Sky Survey IV (Blanton et al. 2017) and DR14 contains an additional  $\sim 100,000$  stars (Abolfathi et al. 2018). The APOGEE instrument is a high-resolution ( $R \sim 22,500$ ) near-infrared ( $1.51\text{-}1.70 \mu\text{m}$ ) spectrograph described in detail in Wilson et al. (in prep). The instrument was connected to the Sloan 2.5m telescope (Gunn et al. 2006) and targets were observed according to Zasowski et al. (2013) for APOGEE, and Zasowski et al. (2017) for APOGEE-2.

The APOGEE data are reduced through methods described by Nidever et al. (2015), and stellar parameters/chemical abundances are extracted using the APOGEE Stellar Parameters and Chemical Abundances Pipeline (ASPCAP, García Pérez et al. 2016). ASPCAP interpolates in a grid of synthetic spectra (Zamora et al. 2015) to find the best fit (through  $\chi^2$  minimization) to the observed spectrum by varying  $T_{\text{eff}}$ , sur-

face gravity, microturbulence, metallicity, carbon abundance, nitrogen abundance, and  $\alpha$ -element abundance. In this analysis we use results from the 14th data release of SDSS (DR14, Abolfathi et al. 2018 and Holtzman et al. 2018). Chemical abundances are derived from lines described in Shetrone et al. (2015). The C and N abundances are derived from features of CO and CN molecules, the data for which come from Pickering (1996) and Sneden et al. (2014), respectively.

In this work, we only analyze APOGEE MW stars that satisfy the following quality cuts to further ensure reliable parameter/abundance derivation:

- $S/N > 80$
- $3500 \text{ K} < T_{\text{eff}} < 5500 \text{ K}$
- $\text{Log}(g) > 1.0$
- No ASPCAPBAD flag set<sup>16</sup>

Uncertainties in the APOGEE chemical abundances are empirically derived by analyzing the abundance scatter in calibration clusters in bins of  $T_{\text{eff}}$ ,  $[M/H]$ , and  $S/N$ . The typical precision of C and N abundances in the parameter space studied in this work is  $\sim 0.03$ - $0.05$  dex. As described further in §3, we divide the APOGEE sample into two groups along the giant branch. The warmer stars residing in the lower part of the giant branch have median C and N uncertainties of 0.04 and 0.06 dex, respectively, resulting in a median  $[C/N]$  uncertainty of 0.07 dex. The cooler stars residing in the upper part of the giant branch have smaller median C and N uncertainties of 0.02 and 0.03 dex, respectively, resulting in a median  $[C/N]$  uncertainty of 0.04 dex. Because of the ASPCAP grid edge, we do not have any stars in our sample with  $[N/Fe] > +1.0$  dex, which may result in the lowest  $[C/N]$  stars dropping out of our sample.

Masses and ages for APOGEE stars analyzed in this work come from Martig et al. (2016b), who used the APOKASC sample (Pinsonneault et al. 2014) to derive a relation between APOGEE DR12 stellar parameters (of which  $[M/H]$  and  $[C/N]$  are the primary drivers) and mass/age, which was then applied to the APOGEE DR12 red giant sample, delivering a catalog of  $\sim 52,000$  APOGEE stars with masses accurate to  $\sim 14\%$  and ages accurate to  $\sim 40\%$ . In this work, we adopt the Martig et al. (2016b) seismic masses and resultant ages for the  $\sim 1,500$  stars in the APOKASC sample to demonstrate that DR14  $[C/N]$  traces mass as DR12  $[C/N]$  did. Distances are derived by methods described in Hayden et al. (2014), and are accurate to  $\sim 20\%$ . For the presentations of our abundance results at various radial zones of the Galaxy, we use standard rectangular Galactic coordinates  $(X, Y, Z)$  where the sun is placed at 8 kpc.

### 3. $[C/N]$ ANALYSIS AND SAMPLE SELECTION

To date, the APOGEE literature works that use  $[C/N]$  abundances as mass/age indicators for red giant stars (e.g., Masseron & Gilmore 2015; Martig et al. 2016b; Ness et al. 2016) have used data from the 12th SDSS data release (DR12, Alam et al. 2015). In this section, we first verify that the newer DR14  $[C/N]$  abundances trace seismic mass in the same way as DR12  $[C/N]$ , and understand across what parameter space this relation is viable. Then we verify that DR14  $[C/N]$  abundances trace stellar ages that are inferred from the seismic masses.

<sup>16</sup> This flag is set if ASPCAP finds an error in deriving any stellar parameters. It is fully described on the DR14 webpages (<http://www.sdss.org/dr14>)

#### 3.1. DR14 $[C/N]$ as a Mass Indicator

The observed atmospheric  $[C/N]$  abundance of a red giant star is the primordial mixture modified by first dredge up, with potential additional mixing that further alters the  $[C/N]$  abundance as a star evolves past the red bump and/or undergoes the helium flash (see e.g. Gratton et al. 2000; Masseron et al. 2017; Lagarde et al. 2018; Shetrone et al. in prep). The extent to which the primordial  $[C/N]$  abundance varies across the Galaxy is not well-understood because it necessitates the study of dwarf and/or subgiant stars that have not yet undergone first dredge up. Martig et al. (2016b) showed that APOGEE subgiant stars, when separated by their location in the Galaxy, exhibited similar  $[C/N]$ - $[Fe/H]$  abundance tracks, suggesting that the primordial  $[C/N]$  abundance variation is small (at least within a few kpc of the Sun). Independent studies of nearby solar twins find a small variation of  $\sim 0.1$  dex in  $[C/Fe]$  (see, e.g., Nissen 2015). This variation is thought to be due to some stars exhibiting deficiencies in refractory elements, potentially a result of planet formation (e.g., Nissen 2015; Spina et al. 2016; Nissen et al. 2017; Bedell et al. 2018). If this is the reason for  $[C/Fe]$  variation, then the  $[C/N]$  abundance ratio should not vary, as C and N have similar condensation temperatures (Lodders 2003). These studies suggest that the  $[C/N]$  variation we observe in the APOGEE red giant stars is likely dominated by mass variation across the Galaxy rather than primordial variation. We further explore how primordial variation might affect our interpretations in §5.2.

Additionally, the  $[C/N]$  abundance ratio of red giant stars may be altered after first dredge up via “extra” metallicity-dependent mixing that takes place as a star evolves along the giant branch past the red bump (see, e.g., Gratton et al. 2000; Shetrone et al. in prep). Lagarde et al. (2018) propose that thermohaline mixing can explain the changing  $[C/N]$  abundance as a star evolves further up the red giant branch. There is also some evidence that the  $[C/N]$  changes when a low-mass star moves in to the core-helium burning red clump (RC) phase after the helium flash (Masseron et al. 2017). Additionally, core-helium burning stars on the RC suffer from higher uncertainties in their asteroseismic masses, and may even suffer from  $[C/N]$  measurement systematics (see, e.g., Tayar et al. 2017). Because of these limitations on  $[C/N]$  as a mass indicator, we divide the APOGEE sample analyzed in this work into two groups along the red giant branch. The lower red giant branch (LGB) sample contains stars with  $2.6 < \log(g) < 3.3$  and the upper red giant branch (UGB) sample contains stars with  $1.0 < \log(g) < 2.1$ . As explained in more detail below, we are more confident that  $[C/N]$  traces mass in the LGB sample, but we include the UGB sample because of its more extensive spatial coverage.

The sample divisions are shown in Figure 1, where we plot DR14  $[C/N]$  as a function of DR14 surface gravity and  $[Fe/H]$  for stars in the APOKASC sample. Points are colored by seismic mass provided in Martig et al. (2016b). Qualitatively, we see that both LGB and UGB samples show a relation between  $[C/N]$  and mass, as seen by the color gradient. The lower cut in  $\log(g)$  of the LGB sample serves to remove the RC stars, which may undergo extra mixing during the helium flash. However, we are sure to include secondary clump stars (2RC) in this sample. The 2RC stars are the most massive stars in our sample, and correspondingly have the lowest  $[C/N]$  values, as seen in the left panel of Figure 1 (red points). Stars with  $M \gtrsim 2.2 M_{\odot}$  spend the majority of their evolved lifetime

as 2RC stars rather than RGB stars, which is likely why there are no massive stars in the UGB sample.

The APOGEE DR14 [C/N]-mass relation is more cleanly seen in Figure 2, where we plot [C/N] vs. APOKASC seismic mass for the LGB (left) and UGB (right) samples described above. The points are colored by [Fe/H]. The LGB stars exhibit a clear correlation between [C/N] and mass for both DR14 and DR12 from  $0.8 < M/M_{\odot} < 2.0$ , indicating that the new DR14 [C/N] abundances can be used as mass indicators for these stars. However, the DR14 [C/N] and [Fe/H] values are slightly lower than the DR12 values (by  $\sim 0.2$  and  $\sim 0.05$  dex, respectively). The relation is relatively weak from  $1.5 < M/M_{\odot} < 2.5$ , suggesting that [C/N] is not a very precise mass indicator for stars of these masses (see Martig et al. 2016b for an in-depth discussion of the [C/N]-mass precision). However, in §4, where we present the results, we are most interested in comparing stars that are either “young”, “intermediate”, or “old” in age, which we can obtain from [C/N].

For the UGB sample, the parameter space is less-sampled, with only two stars with  $\log(g) < 1.5$  and no stars with  $M > 1.7 M_{\odot}$ . Therefore, there is insufficient data to determine whether DR14 [C/N] can be used as a mass indicator for the more luminous red giant stars with  $\log(g) < 1.5$ . However, because the stars that are found in this parameter space do show a relation between [C/N] and mass, we present the [C/N] results for these stars and accompanying age interpretations, as they are valuable tracers of the Galaxy at distances greater than 3 kpc from the Sun. Future studies of potential mixing mechanisms, as well as additional APOKASC observations, will result in a more concrete understanding of whether the [C/N] abundance of stars on the upper giant branch are indicative of their masses.

### 3.2. Mass to Age

In this work we interpret [C/N]-[Fe/H] abundance trends not as mass-[Fe/H] trends, but as age-[Fe/H] trends. The age of a red giant star can be derived from its mass by invoking models of stellar evolution, as was done in Martig et al. (2016b). In the left panel of Figure 3, we plot [C/N] vs.  $\text{Log}(\text{Age}/\text{Gyr})$  derived from the seismic masses by Martig et al. (2016b) for the APOKASC LGB sample. This plot verifies the sensitivity of [C/N] abundance to stellar age. However, for  $\text{Log}(\text{Age}/\text{Gyr}) > 0.3$ , there appears to be a slight color gradient, such that, at fixed age, the metal-poor stars tend to have higher [C/N] than the metal-rich stars. This is because the metallicity of a red giant star affects its age determination, as a more metal-poor star evolves faster through the main-sequence phase than a more metal-rich star of the same mass. This must be taken into account when interpreting the [C/N]-[Fe/H] abundance space as an age-abundance space.

In the right panel of Figure 3, we plot the [C/N]-[Fe/H] abundance space for the APOKASC LGB sample, colored by the age derived by Martig et al. (2016b) from the seismic masses. We divide the sample into a “Young” population, with age  $< 2.5$  Gyr, and an “Old” population with age  $> 9$  Gyr. We bin each sample into 0.1 dex bins of [Fe/H] and fit lines to the median [C/N] values of each bin. These lines show that stars of the same age follow sloped lines in the [C/N]-[Fe/H] abundance plane, which must be taken into consideration when comparing the relative ages of stars at different metallicities using [C/N] as an age indicator. In the following presentation of results, we over-plot these age tracks on the [C/N]-[Fe/H] abundance plots presented in §4, which we use

to guide our interpretation.

## 4. RESULTS

We present the [C/N]-[Fe/H] abundance patterns for the MW Galaxy separately for the LGB and UGB sample. We divide the MW into 6 radial bins of 2 kpc each from 3-15 kpc. We also divide the samples according to height above the plane:  $0 \text{ kpc} < |Z| < 0.5 \text{ kpc}$ ,  $0.5 \text{ kpc} < |Z| < 1.0 \text{ kpc}$ ,  $1.0 \text{ kpc} < |Z| < 2.0 \text{ kpc}$ . In Figures 4 and 9, the points are color-coded by  $\alpha$ -element abundance ( $[\alpha/\text{Fe}]$ ) to explore potential [C/N] differences between the  $\alpha$ -element enhanced and solar- $\alpha$  MW populations, the former of which is generally thought to be older. Medians of [C/N] binned in 0.1 dex bins of [Fe/H] are plotted as black squares.

### 4.1. LGB Sample

The [C/N]-[Fe/H] abundance patterns for the LGB sample are plotted in Figure 4. In each panel, the median [C/N]-[Fe/H] lines corresponding to “Young” and “Old” stars computed in §3.2 are over-plotted as black lines. Because the LGB sample comprises the less luminous giant stars, Galactic coverage is largely limited to 5-13 kpc.

#### 4.1.1. Vertical Trends

The stars with  $[\text{Fe}/\text{H}] > -0.4$  and  $1 \text{ kpc} < |Z| < 2 \text{ kpc}$  have higher [C/N] values than stars in the plane, indicating that these red giant stars are less massive and thus older, on average, than stars in the plane. There also appears to be a slight gradient in mean age from the inner Galaxy to the outer Galaxy for these stars, as the median [C/N] for stars with  $[\text{Fe}/\text{H}] \sim -0.2$  decreases from  $\sim -0.05$  dex in the  $5 \text{ kpc} < R < 7 \text{ kpc}$  bin to  $\sim -0.30$  dex in the  $11 \text{ kpc} < R < 13 \text{ kpc}$  bin. This is qualitatively consistent with the age gradient of  $\sim -0.6$  Gyr/kpc found for the thick disk by Martig et al. (2016a) using DR12 data, and in line with predictions by Minchev et al. (2015), who suggest that the thick disk is a result of an inner disk born hot in a turbulent gas-rich phase, along with the flaring of mono-age stellar populations (see also Mackereth et al. 2017).

The stars that fall in the  $1 \text{ kpc} < |Z| < 2 \text{ kpc}$  and  $7 \text{ kpc} < R < 9 \text{ kpc}$  bin appear to track the “Old” age line which corresponds to a median age of  $\sim 10$  Gyr. As has been shown in the APOGEE data by Hayden et al. (2015), and observed in these data through the coloring of the points, this region of the Galaxy primarily consists of stars enhanced in the  $\alpha$ -elements. The [C/N] abundance trend seems to suggest that the ages of the stars at  $[\text{Fe}/\text{H}] = -0.7$  do not differ significantly from the stars with  $[\text{Fe}/\text{H}] = +0.2$ . This indicates that the evolution of the gas from  $[\text{Fe}/\text{H}] = -0.7$  to  $[\text{Fe}/\text{H}] = +0.2$  happened over a relatively rapid timescale.

While the median [C/N] indicates a relatively constant age with [Fe/H], there is significant dispersion (greater than the 0.07 dex measurement uncertainty) in [C/N] at each metallicity. This is quantified in Figure 5, where we plot the standard deviation of [C/N] in 0.1 dex bins of [Fe/H] for stars around the solar radius (left panel) and just outside the solar radius (right panel) for each  $|Z|$  bin. At the solar radius, the [C/N] dispersion for stars with  $[\text{Fe}/\text{H}] > -0.3$  increases from 0.13 dex to 0.17 dex from out of the plane to in the plane. For stars with  $[\text{Fe}/\text{H}] < -0.3$ , the dispersion is larger overall, but still increases from 0.16 to 0.19 dex from out of the plane to in the plane. The larger scatter in the plane is a consequence of the presence of young, low-[C/N] stars at  $-0.3 < [\text{Fe}/\text{H}] < 0.0$ , which are not found at  $|Z| > 1 \text{ kpc}$ .

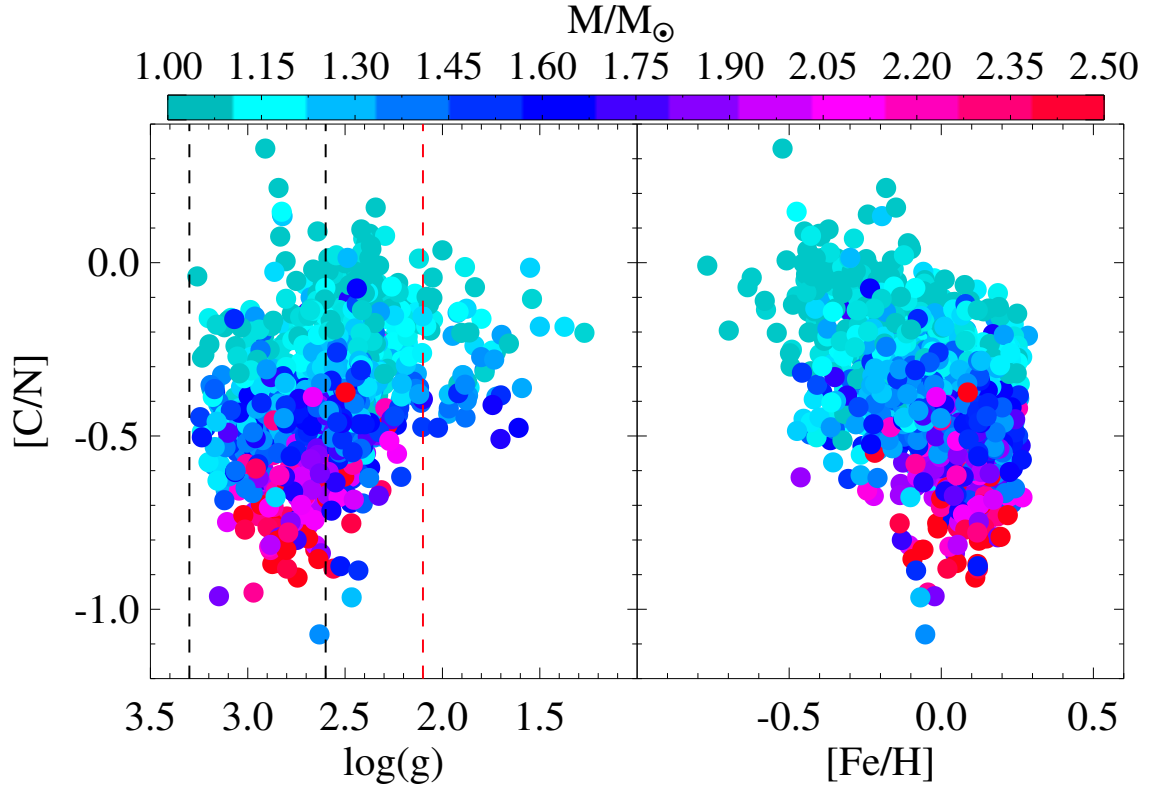


**Figure 1.**  $[\text{C}/\text{N}]$  plotted as a function of  $\log(g)$  (left) and  $[\text{Fe}/\text{H}]$  (right) for stars with seismic masses derived in [Martig et al. \(2016b\)](#). The points are colored by seismic mass, and the black and red dashed lines on the left plots mark the divisions along the giant branch we use to study the abundance patterns of the MW.

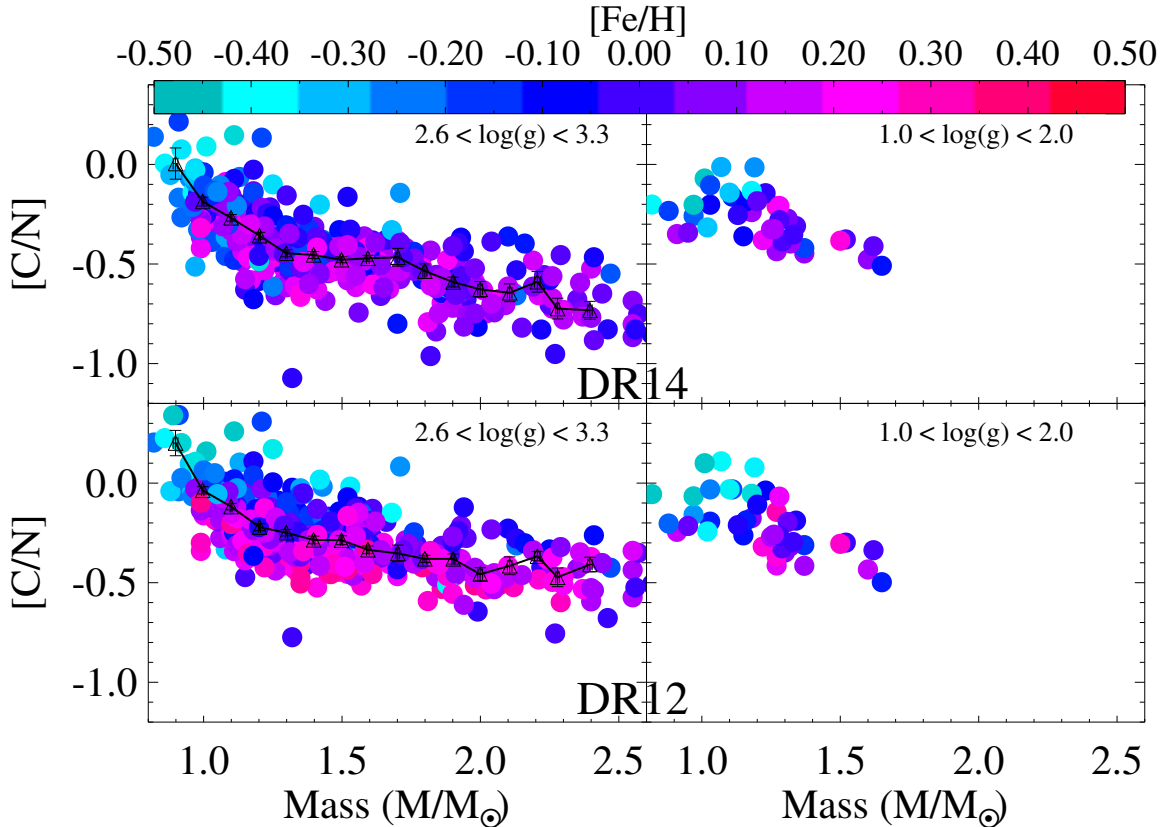


**Figure 2.**  $[\text{C}/\text{N}]$  plotted as a function of seismic mass for both the LGB sample (left) and UGB sample (right). DR14 data are shown in the top row and DR12 data are shown in the bottom row. Points are colored by  $[\text{Fe}/\text{H}]$ . Median  $[\text{C}/\text{N}]$  values binned in mass are plotted as black open triangles.

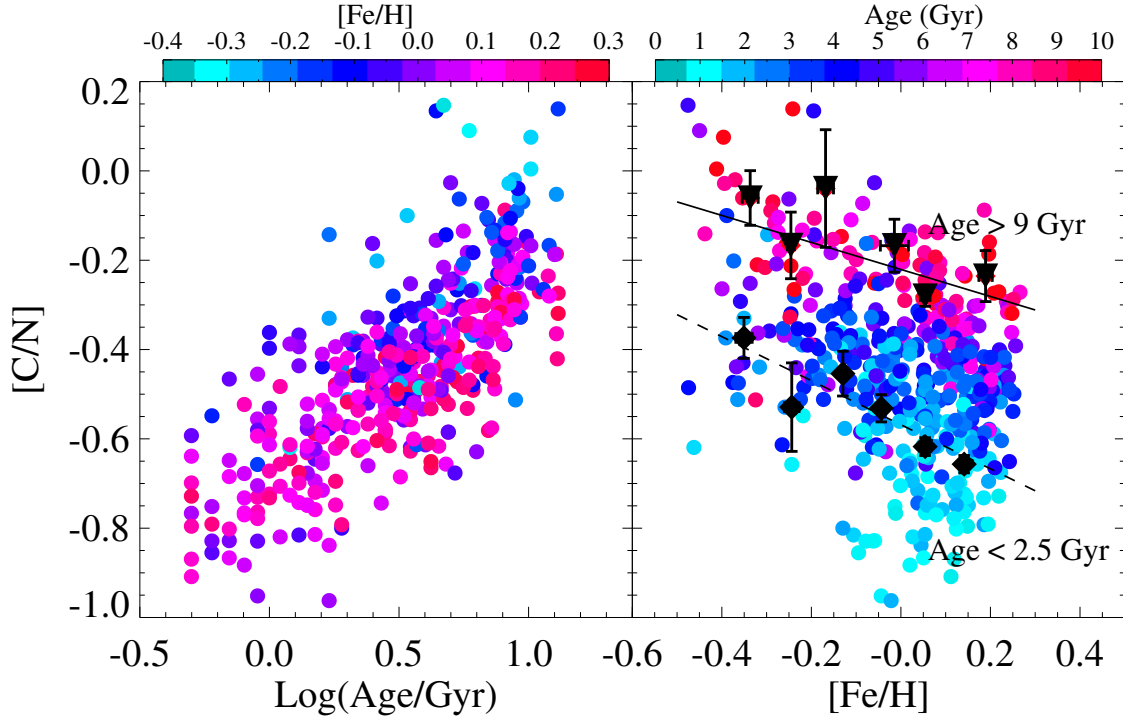


**Figure 3.** Left: [C/N] vs. Log(Age/Gyr) from Martig et al. (2016b) for the APOKASC LGB sample. Points are colored by [Fe/H]. Right: [C/N] vs. [Fe/H] abundance tracks for the same stars in the left panel, colored by the input ages derived by Martig et al. (2016b). The two lines indicate fits to median [C/N] abundances binned by [Fe/H] for stars with asteroseismic ages younger than 2.5 Gyr (black diamonds and dashed line) and older than 9 Gyr (black triangles and solid line).

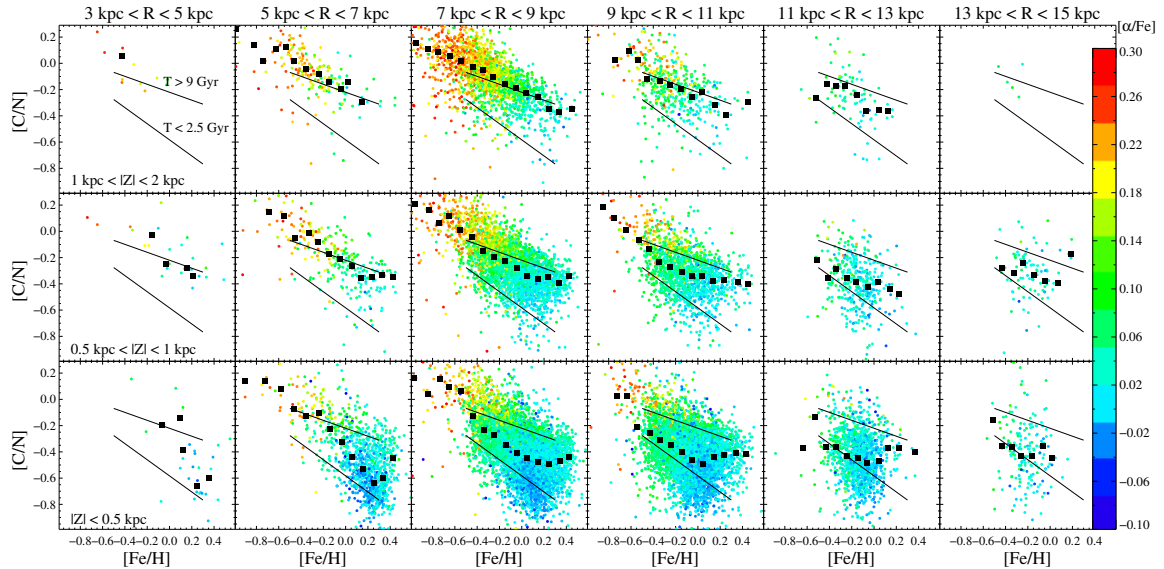


**Figure 4.** [C/N] vs. [Fe/H] abundance patterns for the lower giant branch sample (LGB,  $2.6 < \log(g) < 3.3$ ) across the Galaxy. Points are colored by  $\alpha/\text{Fe}$  and median [C/N] values in bins of [Fe/H] are plotted as black squares. Lines show the tracks for old (age > 9 Gyr) and young (age < 2.5 Gyr) stars from Figure 3.

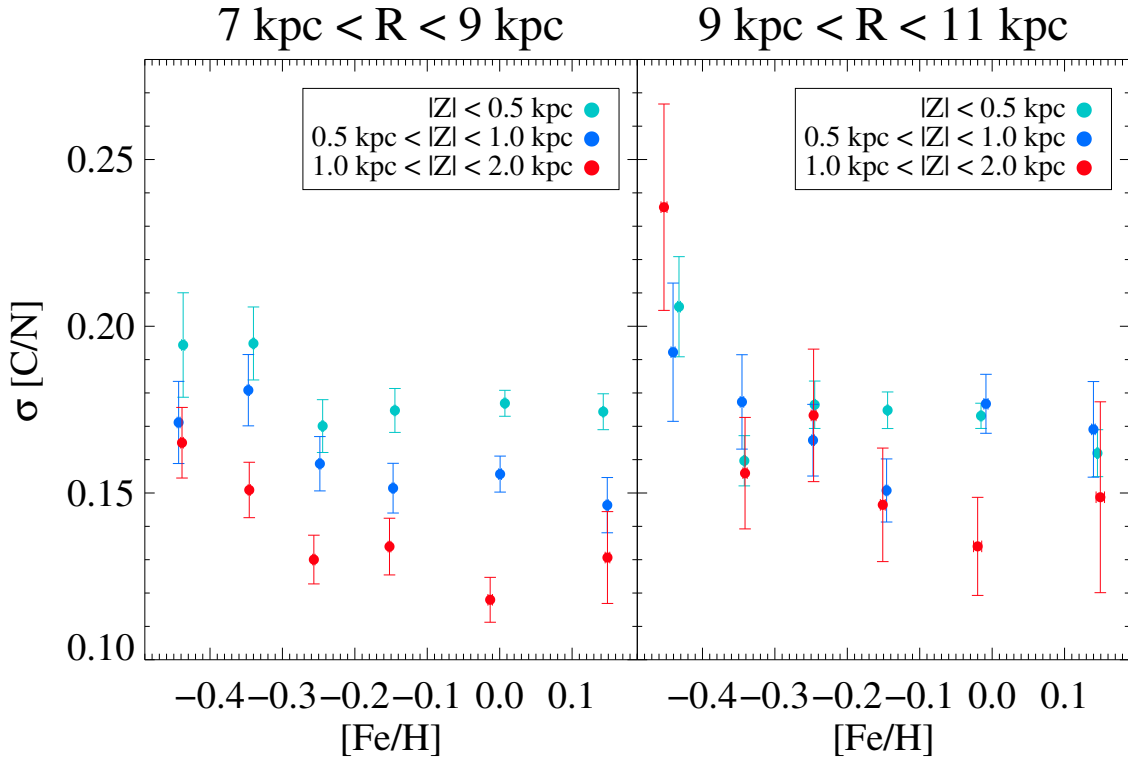


**Figure 5.** The dispersion of [C/N] binned in [Fe/H] for three different heights above the plane for stars with  $7 \text{ kpc} < R < 9 \text{ kpc}$  (left) and  $9 \text{ kpc} < R < 11 \text{ kpc}$  (right). Points are colored by  $|Z|$ , as indicated in the legend.

In the outer disk, the trend of increasing [C/N] dispersion with decreasing  $|Z|$  is less-pronounced, as shown in the right panel of Figure 5. In fact, only stars in the  $[\text{Fe}/\text{H}] = 0.0$  bin show a smaller dispersion of [C/N] out of the plane than in the plane, with all other bins exhibiting similar [C/N] dispersion across all  $|Z|$ . The lack of variation is likely due, in part, to the fact that there are relatively few old, high- $\alpha$  stars populating the disk at  $R > 9 \text{ kpc}$  (see [Nidever et al. 2014](#); [Hayden et al. 2015](#)), which exhibited tighter [C/N] dispersion above the plane at the Solar Neighborhood.

#### 4.1.2. Midplane Radial Trends

The median [C/N] in each radial bin is lower for stars in the plane than stars out of the plane by  $\sim 0.2$  dex, indicating that stars in the plane are generally younger. This is seen in the data through a comparison of the top row of Figure 4 to the bottom row. The  $\alpha$ -element-enhanced stars in the plane generally have higher [C/N] than the solar- $\alpha$  abundance stars in the plane by  $\sim 0.3$  dex at a given [Fe/H], consistent with the  $\alpha$ -element-enhanced stars with  $|Z| > 1 \text{ kpc}$ . Each radial bin in the plane (bottom row of Figure 4) contains stars with [C/N] abundance values that fall  $> 0.2$  dex below the “Young” age line (age  $< 2 \text{ Gyr}$ ). These stars tend to be deficient in  $[\alpha/\text{Fe}]$  by  $\sim 0.1$  dex relative to stars with larger [C/N] abundances at the same [Fe/H]. This correlation between  $\alpha$ -element abundance and [C/N] abundance has been observed in the APOGEE sample before (see, e.g., [Masseron & Gilmore 2015](#); [Ness et al. 2016](#); [Martig et al. 2016b](#)). However, stars with  $-0.4 < [\text{Fe}/\text{H}] < -0.2$  in the Solar Neighborhood exhibit a large spread in [C/N] such that some low- $\alpha$  stars have the same [C/N] abundance as the high- $\alpha$  stars, as can be seen by the coloring of points in Figure 4 in the Solar

Neighborhood bin. Therefore, not only is [Fe/H] a poor tracer of age, as seen by the large spread in [C/N] abundance at a given [Fe/H] abundance, but stars with different  $\alpha$ -element abundances at a given [Fe/H] can be the same age, as suggested by [Mackereth et al. \(2018\)](#).

In the plane, we observe [C/N]-[Fe/H] abundance trends with radius that are not strictly a result of the changing relative amounts of high- $\alpha$  and low- $\alpha$  populations. In the  $5 \text{ kpc} < R < 7 \text{ kpc}$ ,  $|Z| < 0.5 \text{ kpc}$  bin of Figure 4, we observe a smooth decrease of [C/N] with increasing [Fe/H] from  $[\text{Fe}/\text{H}] = -0.6$  to  $[\text{Fe}/\text{H}] = +0.2$ . At  $+0.3 < [\text{Fe}/\text{H}] < +0.5$ , there is an apparent *increase* in median [C/N] from  $[\text{C}/\text{N}] = -0.6$  to  $-0.4$ . We observe such an inflection point in each radial bin (bottom row of Figure 4), but the inflection point (where [C/N] begins to increase rather than decrease) shifts to lower [Fe/H] with increasing radius. In addition to the inflection point becoming more metal-poor, the median [C/N] abundance of the stars with  $+0.2 < [\text{Fe}/\text{H}] < +0.4$  increases with increasing Galactic radius. This is shown in Figure 6 where the [C/N] increases from  $-0.6$  dex to  $-0.4$  dex from 5 kpc to 11 kpc. These trends suggest that at larger Galactic radii ( $R > 9 \text{ kpc}$ ), the metal-rich stars become older than at smaller radii, and can potentially be older than some of the more metal-poor stars in the same radial bin.

The stars with the lowest [C/N] abundance in each radial bin in the plane (bottom row of Figure 4), which likely represent the stars formed in the most recent epoch of star formation in that radial bin, exhibit an apparent anti-correlation between mean [Fe/H] abundance and Galactic radius, indicating there is a negative radial metallicity gradient in the gas participating in star formation in the Galaxy. Additionally, with the exception of the  $11 \text{ kpc} < R < 13 \text{ kpc}$  bin, these low-

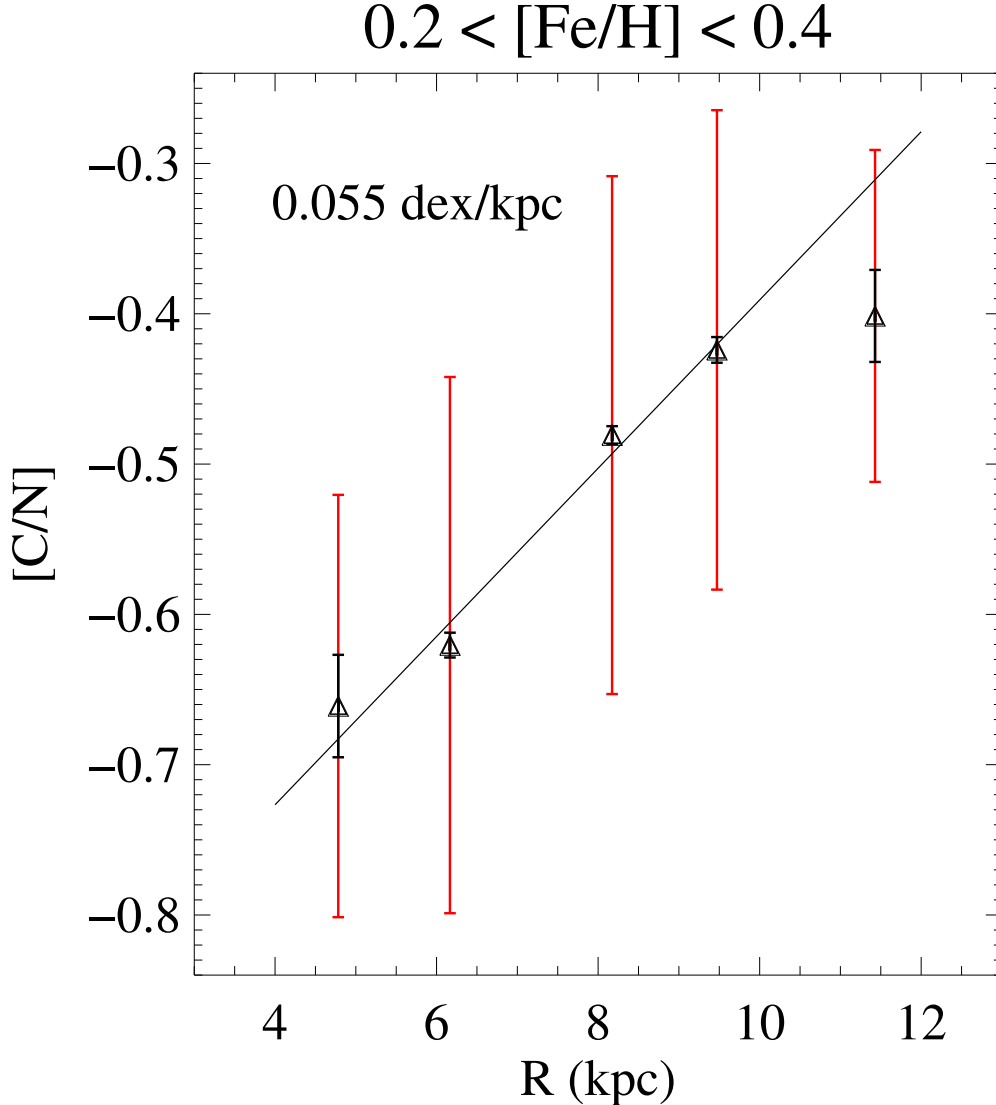


**Figure 6.** Median [C/N] values binned by Galactic radius for stars with  $+0.2 < [\text{Fe}/\text{H}] < +0.4$  for the LGB sample. Black error bars indicate errors on the mean, and red error bars indicate the standard deviation. The errors on the mean are generally quite small ( $< 0.02$  dex), and therefore are not always visible in the plot.

est [C/N], young stars generally exhibit a narrower MDF than stars of larger [C/N] in the same radial bin, as shown in Figure 7, where the MDFs in bins of [C/N] are plotted for the  $|Z| < 0.5$  kpc radial bins. The widths of the MDFs are estimated as the standard deviation of [Fe/H] in each bin, and are listed in each panel of Figure 7. These observations are consistent with MW formation scenarios in which there was a metallicity gradient in the gas participating in star formation across the Galaxy, and this star formation occurs today with gas at one metallicity rather than spanning a range of metallicities. The lack of MDF evolution with [C/N] in the outer Galaxy is likely in part due to the lack of more metal-poor (right-most panel of Figure 7),  $\alpha$ -enhanced stars that are present at  $R < 9$  kpc (see, e.g., Hayden et al. 2015). We explore further interpretations in §5.1.

To quantify the metallicity gradient of the low-[C/N] stars, we plot the median [Fe/H] for the stars with lower [C/N] abundances than the “Young” age track as a function of Galactic radius, shown in the left panel of Figure 8. We fit a line to the medians, weighted by error on the mean, and find that there

is a gradient in [Fe/H] of  $-0.060 \pm 0.002$  dex/kpc for these young stars from 5-12 kpc. Anders et al. (2017) found a gradient of  $-0.057$  dex/kpc for the CoRoGEE stars with ages less than 1 Gyr and  $-0.066$  dex/kpc for the CoRoGEE stars with ages between 1 and 2 Gyr. The gradient found here is also in good agreement with the Genovali et al. (2014) gradient of  $-0.06$  dex/kpc derived from Cepheid stars. It is considerably steeper than work by Balser et al. (2011), who find gradients  $\sim -0.03$ - $0.04$  dex/kpc using metallicities measured from H II regions, but some as high as  $-0.07$  dex/kpc, depending on azimuthal angle. It is also steeper than the gradient found for young planetary nebula by Stanghellini & Haywood (2018) of  $-0.027$  dex/kpc.

Similar gradient analysis with old stars is shown in the right panel of Figure 8. For the older stars we find a flatter gradient of  $-0.016 \pm 0.005$  dex/kpc. This is consistent with what Anders et al. (2017) finds for CoRoGEE stars older than 10 Gyr ( $-0.021$  dex/kpc). This is flatter than the gradients found for old open clusters in the APOGEE data (see, e.g., Cunha et al. 2016), but is consistent with old planetary nebulae mea-



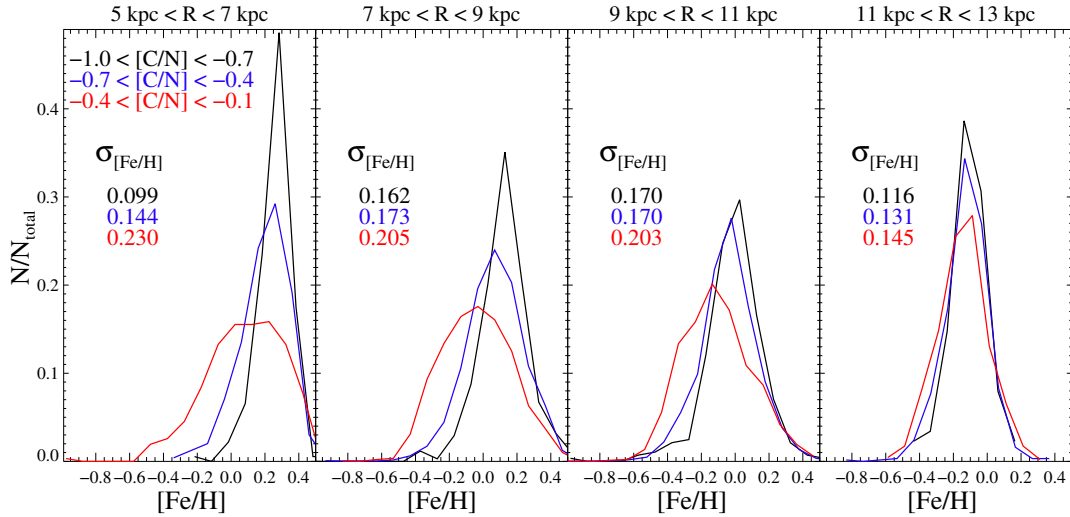


**Figure 7.** MDFs binned by [C/N] for four radial bins for stars with  $|Z| < 0.5$  kpc. The MDFs are colored according to the [C/N] bin, as indicated in the top-left of the left panel, and are normalized to the total number of stars in each bin. The standard deviation of [Fe/H] in each bin is printed in each panel and colored according to [C/N] bin.

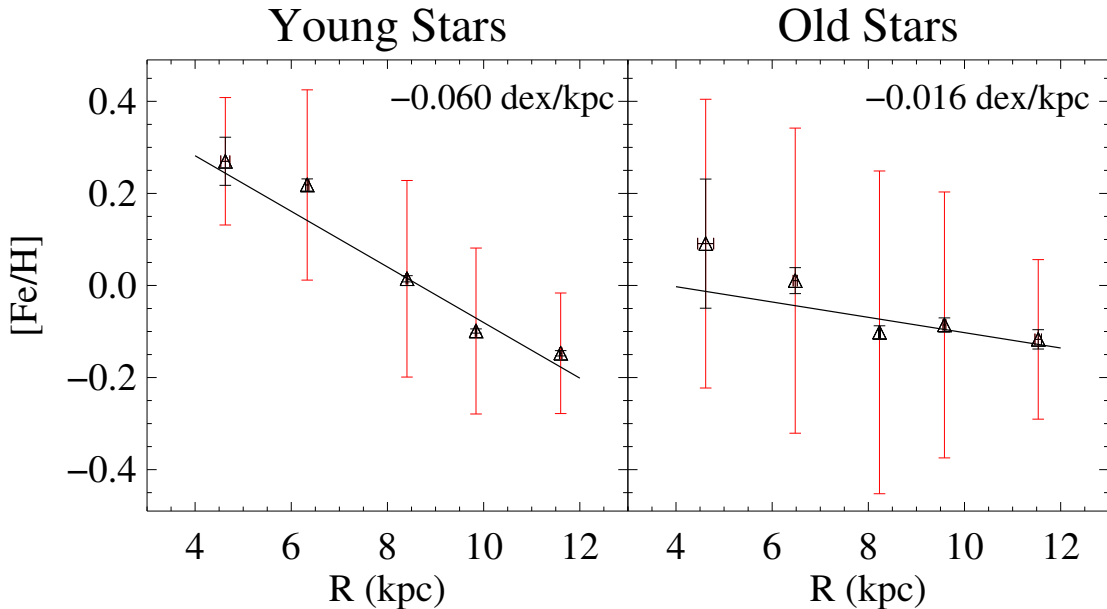


**Figure 8.** Left: Median [Fe/H] values binned by Galactic radius for Young Stars as described in the text. Right: Median [Fe/H] values binned by Galactic radius for Old Stars as described in the text. Black error bars indicate errors on the mean and red error bars indicate standard deviation. The errors on the mean are generally quite small ( $< 0.02$  dex), and therefore are not always visible in the plot.

measurements from [Stanghellini & Haywood \(2018\)](#) of  $-0.015$  dex/kpc. A flattening of the gradient for older stellar populations is predicted by models of Galaxy evolution in which stars migrate over time (see, e.g., [Minchev et al. 2014](#)).

#### 4.2. UGB Sample

The UGB sample traces larger Galactic distances than the LGB sample. However, as explained in §3, there is a lack of APOKASC stars with  $\log(g) < 2.0$  that have seismic masses. Additionally, there are extra-mixing effects that are a function of metallicity and  $\log(g)$ , which can alter the surface [C/N] abundances after the initial, mass-dependent dredge up (see, e.g., [Gilroy 1989](#); [Gratton et al. 2000](#); [Lagarde et al. 2017, 2018](#)). Therefore, it is not clear whether or not the [C/N] abundances for these stars can indicate their age. However, despite these added complications in using [C/N] as a mass in-

dicator, Figure 9 shows that the UGB sample exhibits similar [C/N]-[Fe/H] abundance patterns to the LGB sample where they overlap spatially. In these plots, rather than showing age tracks, we over-plot the median [C/N]-[Fe/H] abundance pattern from the  $7 \text{ kpc} < R < 9 \text{ kpc}$ ,  $|Z| < 0.5$  kpc bin in all other bins so that we can compare other regions of the Galaxy to the Solar Neighborhood. In the following sections, we analyze regions of the Galaxy not probed by the LGB sample, as well as highlight instances where the LGB and UGB [C/N]-[Fe/H] abundances diverge.

##### 4.2.1. Vertical Trends

The UGB sample extends to the  $3 \text{ kpc} < R < 5 \text{ kpc}$  and  $13 \text{ kpc} < R < 15 \text{ kpc}$  bins, which were hardly probed by the LGB sample. Far from the plane ( $1 \text{ kpc} < |Z| < 2 \text{ kpc}$ ), the innermost bin shows a similar [C/N]-[Fe/H] abundance trend

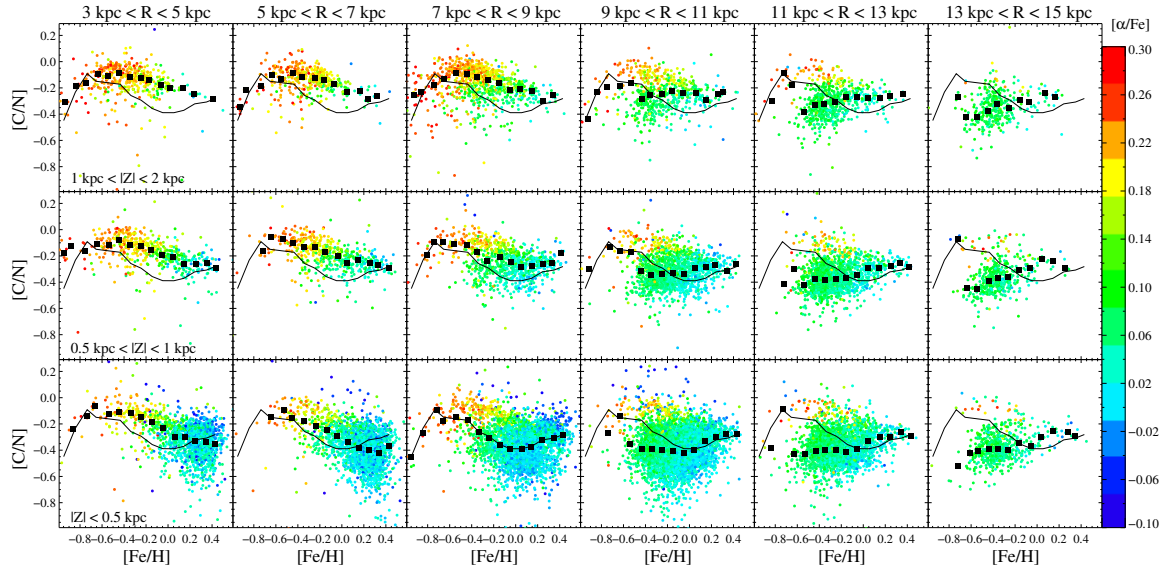


**Figure 9.** Similar to Figure 4 but for the upper giant branch (UGB) stars ( $1.0 < \log(g) < 2.1$ ). Median [C/N] values in bins of [Fe/H] are plotted as black squares. The black line in all panels is a reproduction of the median [C/N] values in bins of [Fe/H] from the  $7 \text{ kpc} < R < 9 \text{ kpc}$ ,  $|Z| < 0.5 \text{ kpc}$  bin.

as the  $5 \text{ kpc} < R < 7 \text{ kpc}$  bin. The outermost bin follows a continuation of the [C/N] gradient where the median [C/N] abundance falls from  $\sim -0.15$  dex to  $\sim -0.35$  dex from 5 kpc to 15 kpc.

The qualitatively similar behavior of the [C/N]-[Fe/H] abundance tracks for the UGB sample at  $[\text{Fe}/\text{H}] > -0.5$  indicates that there is likely still mass information in the [C/N] abundances for these stars. However, at  $[\text{Fe}/\text{H}] < -0.5$ , the [C/N]-[Fe/H] abundance tracks diverge from the LGB sample. The LGB sample showed an anti-correlation between [C/N] and [Fe/H] across the full metallicity range whereas the UGB sample begins to show a *correlation* between [C/N] and [Fe/H] at  $[\text{Fe}/\text{H}] < -0.5$ . This is likely a sign of extra mixing along the giant branch that begins at  $[\text{Fe}/\text{H}] < -0.5$  (see, e.g., Lagarde et al. 2017 and investigated in the APOGEE sample by Shetrone et al. in prep). Additionally, the range in [C/N] values for the UGB sample above the plane and in the  $7 \text{ kpc} < R < 9 \text{ kpc}$  bin is  $\sim 0.4$  dex, whereas the range for the LGB sample at this same Galactic position is  $\sim 0.7$  dex. This suggests that extra mixing occurs along the upper giant branch in such a way that reduces the sensitivity of [C/N] to mass.

At  $R > 11 \text{ kpc}$ , which were regions of the Galaxy not sufficiently probed in the LGB sample, the stars above the plane no longer follow the [C/N]-[Fe/H] anti-correlation, and in fact, exhibit somewhat of a [C/N]-[Fe/H] correlation. As shown in Hayden et al. (2015), and indicated by the coloring of the points in Figure 9, the  $\alpha$ -enhanced stars at  $[\text{Fe}/\text{H}] < -0.2$  no longer occupy this region of the Galaxy. The stars that populate this region of the Galaxy are likely flared “thin-disk” stars. The solar- $\alpha$ ,  $[\text{Fe}/\text{H}] < -0.2$  stars in the outer Galaxy actually exhibit deficient [C/N] relative to the stars with  $[\text{Fe}/\text{H}] > 0.0$  in the same bin by  $\sim 0.1$  dex. This could be an indication that the metal-rich stars in the outer Galaxy are actually older than the more metal-poor stars, a feature that is more pronounced in stars that reside in the plane of the MW and seen in the LGB sample.

#### 4.2.2. Midplane Radial Trends

In the plane, the  $5 \text{ kpc} < R < 7 \text{ kpc}$  bin contains a greater fraction of metal-rich, low-[C/N] stars than the innermost  $3 \text{ kpc} < R < 5 \text{ kpc}$  bin. This is better shown in Figure 10 where

we plot [C/N] distribution functions for the stars with  $+0.2 < [\text{Fe}/\text{H}] < +0.4$ . The distribution in the  $5 \text{ kpc} < R < 7 \text{ kpc}$  is double-peaked, with a peak centered around  $[\text{C}/\text{N}] = -0.5$  that is hardly represented in the  $3 \text{ kpc} < R < 5 \text{ kpc}$  bin. If we take [C/N] to indicate age for the UGB stars, this would suggest that the innermost regions of the Galaxy ( $R < 5 \text{ kpc}$ ) do not have the youngest stars observed in other regions of the Galaxy (particularly the  $5 \text{ kpc} < R < 7 \text{ kpc}$  bin), implying that there has been relatively low star formation in recent times as compared to stars with  $5 \text{ kpc} < R < 9 \text{ kpc}$ .

## 5. INTERPRETATIONS

### 5.1. Chemical Indication of Radial Migration

Based on some Galaxy simulations (see, e.g., Roškar et al. 2008; Bird et al. 2013; Minchev et al. 2013), as well as observations of a change in skewness of the MDFs across the Galaxy presented in Hayden et al. (2015), we expect to see some signature of radial migration in exploring the ages of stellar populations of the MW. Masseron & Gilmore (2015) noticed that there appeared to be a group of super-solar metallicity stars in the APOGEE data with unexpectedly high [C/N]. One explanation for the existence of these metal-rich stars is that they actually formed in the inner Galaxy, where higher ISM metallicities were achieved at earlier times as compared to the outer Galaxy. Over time, via dynamical interactions with the bar and spiral arms, these stars migrated to their present location (see, e.g., Minchev et al. 2013; Kordopatis et al. 2015).

There are two features of radial migration that might manifest themselves in the APOGEE [C/N]-[Fe/H] abundance patterns. First, radial migration scatters stars both ways. Because the outer disk is less-dense than the inner disk, the stars that migrate from in-to-out are expected to make a larger fractional contribution to the stellar populations of the outer disk than stars moving out-to-in (see, e.g., Minchev et al. 2014). Secondly, the older stars will migrate the farthest as they have had more time to migrate. The youngest stars should not have had time to migrate, implying that the metallicity of the youngest stars in a radial bin is a representation of the present-day ISM metallicity in that radial bin. If there are stars more metal-

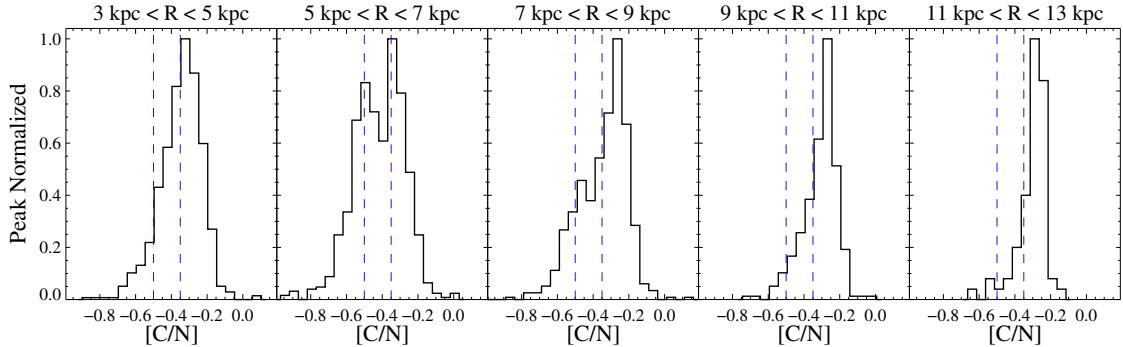


**Figure 10.**  $[C/N]$  histogram for the metal-rich UGB stars ( $1.0 < \log(g) < 2.1$  and  $0.2 < [Fe/H] < 0.4$ ). Only stars with  $|Z| < 0.5$  kpc are plotted. Two fiducial lines meant to roughly track the peaks in the  $5 \text{ kpc} < R < 7 \text{ kpc}$  bin are plotted in each panel.

rich than this metallicity, they might be migrators. To search for signatures of radial migration in the APOGEE data, we look at  $[C/N]$  distributions in bins of  $[Fe/H]$  across the entire Galaxy.

For each radial bin, we define a metallicity of most recent star formation,  $[Fe/H]'$ .  $[Fe/H]'$  is defined as the median metallicity of the 20 stars with the lowest  $[C/N]$  in a given radial bin. For each radial bin, we select stars within 0.1 dex of  $[Fe/H]'$  and analyze their  $[C/N]$  distributions. Without radial migration or the dilution of the ISM via accretion of a significant amount of pristine gas (explored more in §5.3), a simple prediction from chemical evolution would be that the  $[C/N]$  distribution of stars within 0.1 dex of  $[Fe/H]'$  should be skewed heavily towards lower  $[C/N]$  values, or younger ages. In other words, the most-metal rich stars would be the youngest and there would be few old stars that have this same metallicity, as they would have had to form before the ISM was enriched to its current metallicity.

The resulting  $[C/N]$  distributions for different values of  $[Fe/H]'$  across *all* radial bins are shown in Figure 11. In each panel, the  $[Fe/H]'$  considered is shown in the upper right. The dashed line is a fiducial line at  $[C/N] = -0.6$ , which serves as an estimate for indicating young stars. The solid line is the median  $[C/N]$  value in the inner Galaxy, and is the same across each row. The top row shows the  $[C/N]$  distributions for the  $[Fe/H]'$  of the inner Galaxy. At these metallicities, stars are skewed to younger ages in the inner Galaxy, but skewed to older ages in the outer Galaxy. This suggests that the metal-rich stars in the inner Galaxy that have just formed there dominate over older stars that potentially migrated from further in still, whereas the outer Galaxy only contains old metal-rich stars. These features are both consistent with radial migration.

The next row down in Figure 11 shows the  $[C/N]$  distribution of stars with the  $[Fe/H]'$  of the Solar Neighborhood. In the Solar Neighborhood bin, these stars are not skewed to younger ages. In fact, the distribution peaks at a larger value of  $[C/N]$ , indicating that the majority of stars with the  $[Fe/H]'$  of the Solar Neighborhood are actually more of an intermediate age, rather than skewed to younger ages as was the case for the inner Galaxy  $[Fe/H]'$ . This is qualitatively consistent with Minchev et al. (2014) who find that the majority of stars found in the Solar Neighborhood today were not formed there, with  $\sim 60\%$  of the stars arriving from the inner disk. Assuming some of these stars arriving from the inner disk had metallicities similar to the Solar Neighborhood  $[Fe/H]'$ , this would explain the  $[C/N]$  distribution being peaked at larger values. We actually find that the median  $[C/N]$  of stars with Solar Neighborhood  $[Fe/H]'$  peaks at roughly the same place ( $\sim -0.45$ )

across the entire Galaxy studied here. Similar patterns to the Solar Neighborhood  $[Fe/H]'$  distributions are observed in the  $9 \text{ kpc} < R < 11 \text{ kpc}$  bin (third row of Figure 11).

The outermost radial bin shows that the metal-rich stars there are all old, but the stars with the metallicity of the outer Galaxy  $[Fe/H]'$  (bottom row of Figure 11) exhibit a range of  $[C/N]$  values, suggesting a range of ages. This is consistent with radial migration in that the spread of this bin can be attributed to some intermediate age stars that formed in the next bin over ( $9 \text{ kpc} < R < 11 \text{ kpc}$ ) migrating outwards over time. These stars appear to dominate over longer term migrators that may have come from the inner Galaxy at this lower  $[Fe/H]$ .

This interpretation is all based on the assumption that the present day ISM at a given Galactic bin is as metal-rich as it has ever been, and that it was more metal-poor in the past. This may not be true for the Solar Neighborhood, where chemical evolution may have been slow in the past 4.5 Gyr (see e.g. Chiappini et al. 2003). Moreover, some chemical-evolution models show that the ISM can quickly evolve to an “equilibrium abundance”, at which stars are formed over 6-8 Gyr (see, e.g., Andrews et al. 2017; Weinberg et al. 2017). This suggests that a spread in  $[C/N]$  at the  $[Fe/H]'$  of a given radial bin is due to stars forming at this equilibrium abundance over several Gyr, rather than a sign of radial migration. Potential migrators would then be stars that are more metal-poor than the  $[Fe/H]'$  of a given radial bin but younger (e.g., stars with low  $[C/N]$  in the  $[Fe/H] < [Fe/H]'$  panels of the inner Galaxy column in Figure 11). However, since these stars would not have had much time to migrate, they would not be able to stray too far from their birth location. Therefore, an equilibrium abundance scenario would have to explain the presence of metal-poor young stars in a radial bin that’s been forming stars at a much higher metallicity for several Gyr, like we observe in Figure 11.

## 5.2. Primordial Variation

Interpretations presented in this paper are based on the assumption that the observed variation in  $[C/N]$  abundance is dominated by stellar evolution, and is not a reflection of primordial variations in the C and N abundances across the Galaxy. As mentioned earlier, analyses of the Solar Neighborhood have found some slight ( $\sim 0.1$  dex) variations in the  $[C/Fe]$  abundance of solar twins (see, e.g., Nissen 2015), but it is unknown how much the primordial  $[C/N]$  abundance distribution varies across the Galaxy. However, there have been discoveries of chemically anomalous N-enhanced field stars in the APOGEE data (see, e.g., Fernández-Trincado et al. 2016, 2017; Schiavon et al. 2017), which might show up in

## APOGEE [C/N] ABUNDANCES ACROSS THE GALAXY

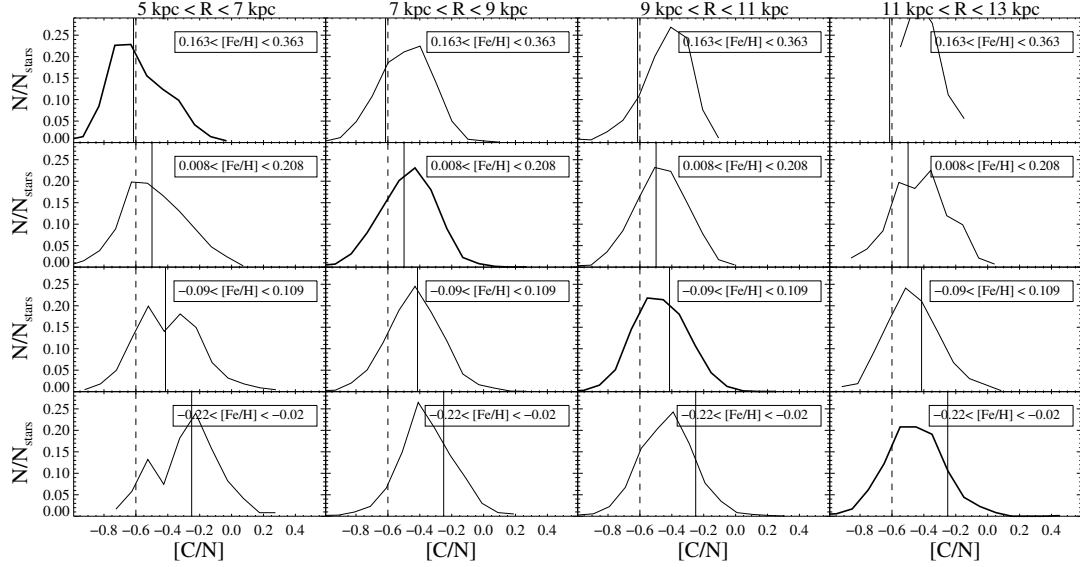


**Figure 11.** [C/N] distributions for stars  $\pm 0.1$  dex from four different [Fe/H] values (indicated in the upper right of each panel) from the inner Galaxy to the outer Galaxy (columns, with radial range as marked). The four [Fe/H] values correspond to the median metallicity of the most recently formed stars (specifically, of the 20 stars with the lowest [C/N]) in each radial bin. The solid line marks the median [C/N] of the inner Galaxy bin, and is the same across each row. The dashed line is a fiducial line at [C/N] =  $-0.6$ , which serves as an estimate for indicating young stars.

our sample as low-[C/N] stars. These stars are few in number (11 found in the disk), and generally exhibit  $[\text{Fe}/\text{H}] < -0.5$ , so their contribution to the gradient and migration analysis is likely insignificant.

In addition to anomalous field stars being present, different star-formation histories of the inner and outer disk might result in variation of the primordial [C/N] abundance. For example, [Bensby et al. \(2005\)](#) found signs of *s*-process enrichment in the Galactic thin disk around the Solar Neighborhood, which suggests that AGB stars might be important contributors to the formation of these stars. In the inner Galaxy, where the chemical enrichment was more rapid, Type II SNe likely dominated the chemical enrichment without much time for AGB stars to contribute. If the AGB stars contribute additional C and/or N relative to Fe, then the metal-rich stars in the outer Galaxy may simply have been formed with a different primordial [C/N] abundance than the inner Galaxy. [Masseron & Gilmore \(2015\)](#) found that the APOGEE data exhibited an increase in  $[(\text{C}+\text{N})/\text{Fe}]$  with increasing [Fe/H] above solar metallicities, which they attributed to potential AGB enrichment.

In [Figure 12](#) we plot the  $[(\text{C}+\text{N})/\text{Fe}]$  vs. [Fe/H] abundance tracks for the LGB sample, this time colored by [C/N], to investigate potential differences in the  $[(\text{C}+\text{N})/\text{Fe}]$  abundance patterns between the inner and outer Galaxy that may affect our [C/N]-age interpretations. We find that the stars with  $|Z| > 1$  kpc have larger  $[(\text{C}+\text{N})/\text{Fe}]$  abundances than the stars in the plane at  $[\text{Fe}/\text{H}] \sim -0.2$ , but are mostly similar at other metallicities. This is akin to the  $\alpha$ -element abundance differences, and is consistent with the  $\alpha$ -element enhanced stars having formed with a larger relative amount of Type II SNe ejecta. At super-solar [Fe/H], we see the same increase of  $[(\text{C}+\text{N})/\text{Fe}]$  with [Fe/H] that [Masseron & Gilmore \(2015\)](#) observed, but we observe this trend in every radial/Z bin. The fiducial line from the Solar Neighborhood indicates that there is little variation in this trend between bins. This suggests that whatever process (or processes) causes an increase in  $[(\text{C}+\text{N})/\text{Fe}]$  with increasing [Fe/H] at  $[\text{Fe}/\text{H}] > 0.0$  operates in a similar fashion between the inner Galaxy and outer Galaxy.

We investigated the same tracks for the UGB sample and found similar results. All Galactic zones show an increase in  $[(\text{C}+\text{N})/\text{Fe}]$  with increasing [Fe/H] at super-solar metallicities.

We take this one step further by analyzing the [C/N] and  $[(\text{C}+\text{N})/\text{Fe}]$  distributions of the inner Galaxy and outer Galaxy for a small section in [Fe/H] ( $+0.2 < [\text{Fe}/\text{H}] < +0.3$ ). The left panel of [Figure 13](#) illustrates the different [C/N] distributions between the inner and outer Galaxy for the LGB sample, which we described as a sign of radial migration. The middle panel suggests that there may be a slight difference in the means of the two  $[(\text{C}+\text{N})/\text{Fe}]$  distributions, however, when splitting the stars by [C/N] instead of radius, we see that both the low-[C/N] and high-[C/N] stars exhibit this trend of increasing  $[(\text{C}+\text{N})/\text{Fe}]$  with increasing [Fe/H]. This again suggests that the  $[(\text{C}+\text{N})/\text{Fe}]$  increase is mostly decoupled from the [C/N] abundance patterns.

If we interpret [C/N] as an age indicator, then both old and young stars show an increase in  $[(\text{C}+\text{N})/\text{Fe}]$  with increasing [Fe/H]. This likely rules out both intermediate-mass and low-mass AGB ejecta as the source of this increase, as the timescales for enrichment are too long to contribute to the enrichment of the older stellar populations found in the inner Galaxy. Moreover, AGB yields from [Karakas & Lugaro \(2016\)](#) actually suggest that the solar-metallicity models produce more C and N relative to Fe than the super-solar metallicity models, although more massive AGB stars produce more C and N relative to Fe than less-massive AGB stars. They also note that it is unlikely intermediate-mass AGB stars contributed significantly to the chemical evolution of the MW disk. [Henry et al. \(2018\)](#) calls this into question, noting that they find larger N/O abundance ratios in their observations of PNe than most models predict, but this enhancement does not appear to be a function of metallicity. However, [van Zee et al. \(1998\)](#) finds an increase of N/O with O/H in H II regions, which indicates that metal-rich Type II SNe begin to add nitrogen that would cause an increase in the total  $[(\text{C}+\text{N})/\text{Fe}]$ . This latter scenario would explain the observed increase in  $[(\text{C}+\text{N})/\text{Fe}]$  with increasing [Fe/H] observed in both the inner

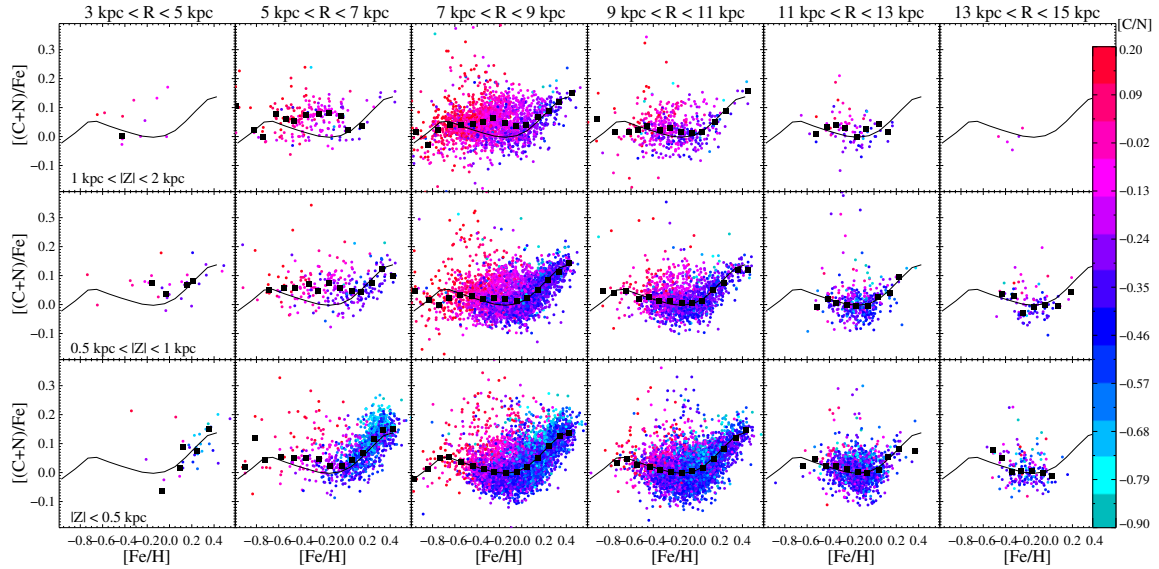


**Figure 12.**  $[(C+N)/Fe]$  for the lower giant branch stars ( $2.6 < \log(g) < 3.3$ ). Points are color-coded by  $[C/N]$  abundance. Medians binned in  $[Fe/H]$  are plotted as black squares. A fiducial line from the Solar Neighborhood,  $|Z| > 0.5$  kpc bin is plotted in all panels.

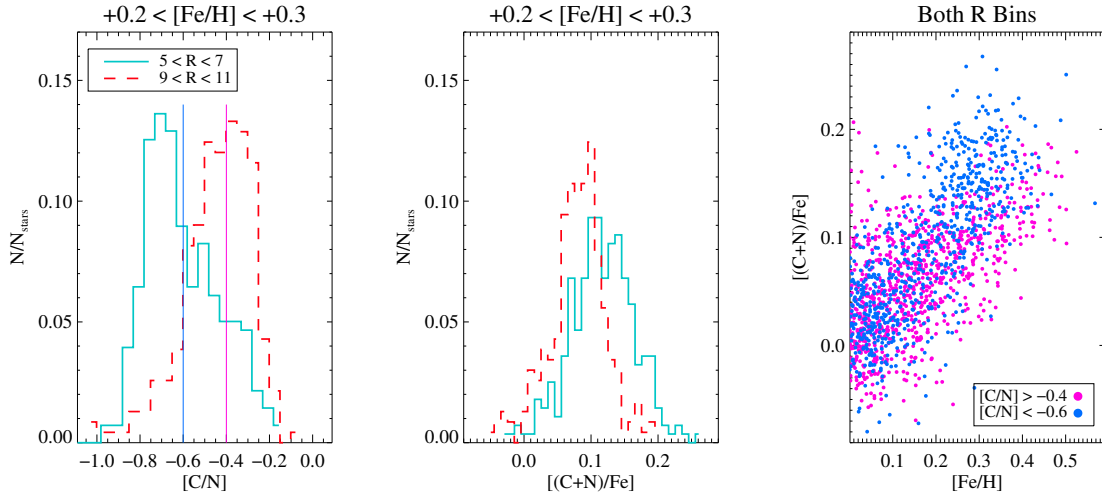


**Figure 13.** Elemental distributions for the LGB sample with  $|Z| < 0.5$  kpc. Left:  $[C/N]$  distribution for the  $5 \text{ kpc} < R < 7 \text{ kpc}$  bin (blue) and the  $9 \text{ kpc} < R < 11 \text{ kpc}$  bin (red) for stars with  $+0.2 < [Fe/H] < +0.3$ . Middle: same as left but for  $[(C+N)/Fe]$ . Right:  $[(C+N)/Fe]$  vs.  $[Fe/H]$  for the two combined bins, but separated at  $[C/N] > -0.4$  (orange) and  $[C/N] < -0.6$  (cyan), indicated in the left plot by the vertical lines.

and outer Galaxy.

### 5.3. Two-Infall or Major Merger

Metal-rich old stars at the same Galactic radius as metal-poor young stars could, in principle, be a result of two major gas accretion events in the MW’s history that were each followed by an epoch of star formation. The first epoch is a vigorous star-formation event spurred by an initial infall of gas that forms the high- $\alpha$  sequence of stars out to some radius. Then, there is a break in star formation followed by the accretion of gas that has been polluted in part by SNe from previous star-formation events (e.g., a “Galactic Fountain”, Marasco et al. 2013), but also sufficiently diluted by pristine gas such that it is more metal-poor (but still solar-like  $\alpha$ -element abundance) than stars that had already formed in the MW. This results in younger stars being more metal-poor than the older metal-rich stars formed at the end of the first major star formation epoch that happen to reside at the same

Galactic radius. A decrease of gas-phase metallicity with time can also arise in a chemical-evolution model with outflows, if the outflow efficiency increases with time (see, e.g., Fig. 9 of Weinberg et al. 2017).

Recent results from Grand et al. (2018) suggest that low- $\alpha$ , low- $[Fe/H]$  stars can form in the outer Galaxy if an initial epoch of star formation is followed by a paucity of star formation which results in a shrinkage of the gaseous disk to a smaller radius than the radius where it previously formed stars. Future accretion of pristine gas then mixes with Type Ia SNe remnant material which could, in principle, then form stars at a lower metallicity than the initial epoch of star formation. Mackereth et al. (2018) similarly find that such a star-formation history can give rise to the observed  $[\alpha/Fe]$  bimodality. However, they find that the median  $[Fe/H]$  of both the high- $\alpha$  and low- $\alpha$  sequence increases with time, implying that it is migration that causes the observed flattening of the age-metallicity relation in the MW. Studies of the MW

disk using the entire suite of APOGEE chemical abundances (which is beyond the scope of this paper) will shed more light on the two-infall scenario, and answer whether this scenario might naturally explain the observed [C/N]-[Fe/H] abundance trends, or if significant migration is indeed required.

It is also possible that the old, metal-rich stars that are found throughout the Galactic disk are a result of a major merger of a relatively massive galaxy that was able to enrich its ISM to super-solar metallicities before merging with the MW. However, because these stars are as metal-rich as  $[\text{Fe}/\text{H}] \sim +0.3$ - $+0.4$ , such a galaxy would likely either have had to have been more massive than the LMC, or had an exotic star formation history such that it was able to enrich its gas to much higher metallicities than would be predicted by its mass based on the observed mass-metallicity relation of galaxies observed today (e.g., Kirby et al. 2013). The former scenario would then argue that the MW disk contains a large fraction (10+%) of stars coming from a major merger.

#### 5.4. Measurement Systematics

In a recent comparison of the APOGEE abundances to optical abundances for an overlapping sample of stars, Jönsson et al. (2018) found that the difference between APOGEE [N/Fe] abundances and optical [N/Fe] abundances (from da Silva et al. 2015 and Brewer et al. 2016) increases with increasing [Fe/H] such that the APOGEE [N/Fe] are  $\sim 0.2$ - $0.3$  dex higher at  $[\text{Fe}/\text{H}] > 0.3$ . While the APOGEE spectral region contains many more CN lines from which N abundances can be derived than the optical, it is not conclusive whether the APOGEE abundances or the optical abundances are systematically off. Such a systematic could be responsible for the increase of  $[(\text{C}+\text{N})/\text{Fe}]$  with [Fe/H] seen in §5.2, and observed by Masseron & Gilmore (2015) in DR12. However, this potential measurement systematic would not explain the outer Galaxy stars being preferentially high in [C/N] but the inner Galaxy stars exhibiting a range in [C/N] at the same metallicity.

## 6. CONCLUSIONS

We have presented APOGEE [C/N]-[Fe/H] abundance trends across much of the Galactic disk (3-15 kpc). Similar to other studies of APOGEE [C/N] abundances, we demonstrate that these abundance trends can be interpreted as age-[Fe/H] trends, allowing for the temporal exploration of the chemical evolution of the MW Galaxy.

The APOGEE LGB sample exhibits significant scatter in [C/N], which we interpret as scatter in age, across all metallicities in all regions of the Galactic disk. Therefore, we conclude that there is no age-metallicity relation in any part of the MW disk explored in this work. The [C/N] dispersion for stars with  $[\text{Fe}/\text{H}] > -0.3$  increases from 0.13 dex to 0.17 dex from out of the plane to in the plane. The increase is driven by the inclusion of the youngest stars (age  $< 2.5$  Gyr) that are only found in the plane.

Far from the plane ( $|Z| > 1$  kpc), we observe a gradient in the mean [C/N] of stars of  $-0.04$  dex/kpc from 6-12 kpc, implying that the stars far from the plane become younger from inner to outer Galaxy. This is similar to the age gradient of the thick disk found by Martig et al. (2016a), and consistent with the prediction of Minchev et al. (2015), who show that such an age gradient in a thick disk is expected if the thick disk is a result of the flaring of mono-age populations. In the plane ( $|Z| < 0.5$  kpc), there is a radial [Fe/H] gradient of the

youngest stars of  $-0.060$  dex/kpc, whereas the older stars exhibit a much flatter gradient of  $-0.016$  dex/kpc. Both of these gradients are consistent with what Anders et al. (2017) measured using the CoRoGEE sample. Such a flattening of the [Fe/H] gradient of the disk with time is predicted by Minchev et al. (2013) to be a consequence of radial heating and migration.

The UGB sample, which consists of stars with lower surface gravity that are few in number in the APOKASC catalog, appear to follow [C/N]-[Fe/H] abundance trends that are similar to those of the LGB sample. Notable differences are the smaller overall range in [C/N] as well as the [C/N]-[Fe/H] correlation for stars with  $[\text{Fe}/\text{H}] < -0.6$ , which is not observed in the LGB sample. This latter observation is likely due to extra metallicity-dependent mixing that occurs as a star evolves further up the giant branch. We find that the metal-rich stars ( $[\text{Fe}/\text{H}] > +0.2$ ) that reside in the  $5 \text{ kpc} < R < 7 \text{ kpc}$  bin are much younger, on average, than stars in the  $3 \text{ kpc} < R < 5 \text{ kpc}$  bin. This suggests that the inner Galaxy is experiencing relatively little star formation as compared to the rest of the disk, or that the inner disk is dominated by old stars.

In the LGB and UGB sample, we also observe an upturn in the [C/N]-[Fe/H] abundance trends in the plane for  $R > 7$  kpc. This upturn is a consequence of the metal-rich stars ( $[\text{Fe}/\text{H}] > +0.2$ ) in the outer Galaxy exhibiting larger [C/N] values than more metal-poor stars in the same bin, suggesting they are older. Conversely, these metal-rich stars in the inner Galaxy exhibit a range of ages, but are skewed towards younger ages. It is plausible that radial migration is responsible for the presence of the metal-rich stars in the outer Galaxy that are  $\sim 0.3$ - $0.4$  dex more metal-rich than the metallicity of the youngest stars in the outer Galaxy. Additionally, the [C/N] distributions of the Solar Neighborhood, which are peaked at intermediate ages across a range of metallicities (including the metallicity of the present-day Solar Neighborhood ISM), suggest that a majority of stars in the Solar Neighborhood formed farther in and migrated outward to the Solar Neighborhood. This is qualitatively consistent with the predicted distribution of birth and final radii from Minchev et al. (2014).

We have also explored other possible explanations for the observed [C/N]-[Fe/H] abundance trends. The large dispersion in [C/N]/age at fixed metallicity could be a consequence of a Galactic ISM that does not evolve substantially in metallicity over the past  $\sim 4$ - $6$  Gyr, rather than radial migration. This could explain the large scatter in the ages of stars at solar metallicity in the Solar Neighborhood, but a mechanism like radial migration would still need to be invoked to explain the intermediate age stars that are 0.2-0.3 dex more metal-poor than the young metal-rich stars forming in the inner Galaxy, as well as the old metal-rich stars in the outer Galaxy. We also explore whether the [C/N]-[Fe/H] abundance pattern is a result of primordial variation by analyzing the  $[(\text{C}+\text{N})/\text{Fe}]$  abundance, which is a quantity that should be conserved during stellar evolution, and is therefore indicative of a primordial  $[(\text{C}+\text{N})/\text{Fe}]$  abundance. We do find that there is an increase of  $[(\text{C}+\text{N})/\text{Fe}]$  with [Fe/H] at super-solar metallicities, but this increase occurs across the entire Galaxy and for all values of [C/N], suggesting that whatever is causing the increase in  $[(\text{C}+\text{N})/\text{Fe}]$  does not significantly alter the [C/N] abundance. However, studies of C and N abundances of dwarf/subgiant stars across the entire Galaxy is necessary to properly quantify the primordial variation of [C/N].

*Acknowledgments.*

We thank the anonymous referee for their insightful comments that really helped to improve this manuscript.

Funding for the Sloan Digital Sky Survey IV has been provided by the Alfred P. Sloan Foundation, the U.S. Department of Energy Office of Science, and the Participating Institutions. SDSS acknowledges support and resources from the Center for High-Performance Computing at the University of Utah. The SDSS web site is [www.sdss.org](http://www.sdss.org).

SDSS is managed by the Astrophysical Research Consortium for the Participating Institutions of the SDSS Collaboration including the Brazilian Participation Group, the Carnegie Institution for Science, Carnegie Mellon University, the Chilean Participation Group, the French Participation Group, Harvard-Smithsonian Center for Astrophysics, Instituto de Astrofísica de Canarias, The Johns Hopkins University, Kavli Institute for the Physics and Mathematics of the Universe (IPMU) / University of Tokyo, Lawrence Berkeley National Laboratory, Leibniz Institut für Astrophysik Potsdam (AIP), Max-Planck-Institut für Astronomie (MPIA Heidelberg), Max-Planck-Institut für Astrophysik (MPA Garching), Max-Planck-Institut für Extraterrestrische Physik (MPE), National Astronomical Observatory of China, New Mexico State University, New York University, University of Notre Dame, Observatório Nacional / MCTI, The Ohio State University, Pennsylvania State University, Shanghai Astronomical Observatory, United Kingdom Participation Group, Universidad Nacional Autónoma de México, University of Arizona, University of Colorado Boulder, University of Oxford, University of Portsmouth, University of Utah, University of Virginia, University of Washington, University of Wisconsin, Vanderbilt University, and Yale University.

D. A. G. H. and O. Z. acknowledge support provided by the Spanish Ministry of Economy and Competitiveness (MINECO) under grant AYA-2017-88254-P. T.C.B. acknowledges partial support for this work from grant PHY 14-30152; Physics Frontier Center/JINA Center for the Evolution of the Elements (JINA-CEE), awarded by the US National Science Foundation.

## REFERENCES

- Abolfathi, B., Aguado, D. S., Aguilar, G., et al. 2018, *ApJS*, 235, 42
- Alam, S., Albareti, F. D., Allende Prieto, C., et al. 2015, *ApJS*, 219, 12
- Anders, F., Chiappini, C., Santiago, B. X., et al. 2018, *ArXiv e-prints*, arXiv:1803.09341
- Anders, F., Chiappini, C., Minchev, I., et al. 2017, *A&A*, 600, A70
- Andrews, B. H., Weinberg, D. H., Schönrich, R., & Johnson, J. A. 2017, *ApJ*, 835, 224
- Balsler, D. S., Rood, R. T., Bania, T. M., & Anderson, L. D. 2011, *ApJ*, 738, 27
- Bedell, M., Bean, J. L., Melendez, J., et al. 2018, *ArXiv e-prints*, arXiv:1802.02576
- Bensby, T., Feltzing, S., & Lundström, I. 2004, *A&A*, 421, 969
- Bensby, T., Feltzing, S., Lundström, I., & Ilyin, I. 2005, *A&A*, 433, 185
- Bird, J. C., Kazantidis, S., Weinberg, D. H., et al. 2013, *ApJ*, 773, 43
- Blanton, M. R., Bershady, M. A., Abolfathi, B., et al. 2017, *AJ*, 154, 28
- Brewer, J. M., Fischer, D. A., Valenti, J. A., & Piskunov, N. 2016, *ApJS*, 225, 32
- Carlberg, R. G., Dawson, P. C., Hsu, T., & Vandenberg, D. A. 1985, *ApJ*, 294, 674
- Chiappini, C., Anders, F., & Minchev, I. 2014, in *EAS Publications Series*, Vol. 67, *EAS Publications Series*, 169–176
- Chiappini, C., Romano, D., & Matteucci, F. 2003, *MNRAS*, 339, 63
- Chiappini, C., Anders, F., Rodrigues, T. S., et al. 2015, *A&A*, 576, L12
- Cunha, K., Frinchaboy, P. M., Souto, D., et al. 2016, *Astronomische Nachrichten*, 337, 922
- da Silva, R., Milone, A. d. C., & Rocha-Pinto, H. J. 2015, *A&A*, 580, A24
- Edvardsson, B., Andersen, J., Gustafsson, B., et al. 1993, *A&A*, 275, 101
- Eisenstein, D. J., Weinberg, D. H., Agol, E., et al. 2011, *AJ*, 142, 72
- Fernández-Trincado, J. G., Robin, A. C., Moreno, E., et al. 2016, *ApJ*, 833, 132
- Fernández-Trincado, J. G., Zamora, O., García-Hernández, D. A., et al. 2017, *ApJL*, 846, L2
- Feuillet, D. K., Bovy, J., Holtzman, J., et al. 2016, *ApJ*, 817, 40
- . 2018, *MNRAS*, 477, 2326
- Fuhrmann, K. 2008, *MNRAS*, 384, 173
- García Pérez, A. E., Allende Prieto, C., Holtzman, J. A., et al. 2016, *AJ*, 151, 144
- Genovali, K., Lemasle, B., Bono, G., et al. 2014, *A&A*, 566, A37
- Gilroy, K. K. 1989, *ApJ*, 347, 835
- Grand, R. J. J., Bustamante, S., Gómez, F. A., et al. 2018, *MNRAS*, 474, 3629
- Gratton, R. G., Sneden, C., Carretta, E., & Bragaglia, A. 2000, *A&A*, 354, 169
- Gunn, J. E., Siegmund, W. A., Mannery, E. J., et al. 2006, *AJ*, 131, 2332
- Hayden, M. R., Holtzman, J. A., Bovy, J., et al. 2014, *AJ*, 147, 116
- Hayden, M. R., Bovy, J., Holtzman, J. A., et al. 2015, *ApJ*, 808, 132
- Haywood, M., Di Matteo, P., Lehnert, M. D., Katz, D., & Gómez, A. 2013, *A&A*, 560, A109
- Henry, R. B. C., Stephenson, B. G., Miller Bertolami, M. M., Kwitter, K. B., & Balick, B. 2018, *MNRAS*, 473, 241
- Holtzman, J. A., Hasselquist, S., Shetrone, M., et al. 2018, *AJ*, 156, 125
- Iben, Jr., I. 1965, *ApJ*, 142, 1447
- Jönsson, H., Allende Prieto, C., Holtzman, J. A., et al. 2018, *AJ*, 156, 126
- Karakas, A. I., & Lugaro, M. 2016, *ApJ*, 825, 26
- Kirby, E. N., Cohen, J. G., Guhathakurta, P., et al. 2013, *ApJ*, 779, 102
- Kordopatis, G., Binney, J., Gilmore, G., et al. 2015, *MNRAS*, 447, 3526
- Lagarde, N., Robin, A. C., Reylé, C., & Nasello, G. 2017, *A&A*, 601, A27
- Lagarde, N., Reylé, C., Robin, A. C., et al. 2018, *ArXiv e-prints*, arXiv:1806.01868
- Lodders, K. 2003, *ApJ*, 591, 1220
- Loebman, S. R., Debattista, V. P., Nidever, D. L., et al. 2016, *ApJL*, 818, L6
- Loebman, S. R., Roškar, R., Debattista, V. P., et al. 2011, *ApJ*, 737, 8
- Mackereth, J. T., Crain, R. A., Schiavon, R. P., et al. 2018, *MNRAS*, 477, 5072
- Mackereth, J. T., Bovy, J., Schiavon, R. P., et al. 2017, *ArXiv e-prints*, arXiv:1706.00018
- Majewski, S. R., Schiavon, R. P., Frinchaboy, P. M., et al. 2017, *AJ*, 154, 94
- Marasco, A., Marinacci, F., & Fraternali, F. 2013, *MNRAS*, 433, 1634
- Martig, M., Minchev, I., Ness, M., Fouesneau, M., & Rix, H.-W. 2016a, *ApJ*, 831, 139
- Martig, M., Rix, H.-W., Silva Aguirre, V., et al. 2015, *MNRAS*, 451, 2230
- Martig, M., Fouesneau, M., Rix, H.-W., et al. 2016b, *MNRAS*, 456, 3655
- Masseron, T., & Gilmore, G. 2015, *MNRAS*, 453, 1855
- Masseron, T., Lagarde, N., Miglio, A., Elsworth, Y., & Gilmore, G. 2017, *MNRAS*, 464, 3021
- Minchev, I., Chiappini, C., & Martig, M. 2013, *A&A*, 558, A9
- Minchev, I., Chiappini, C., & Martig, M. 2014, *A&A*, 572, A92
- Minchev, I., Martig, M., Streich, D., et al. 2015, *ApJL*, 804, L9
- Minchev, I., Steinmetz, M., Chiappini, C., et al. 2017, *ApJ*, 834, 27
- Minchev, I., Anders, F., Recio-Blanco, A., et al. 2018, *ArXiv e-prints*, arXiv:1804.06856
- Ness, M., Hogg, D. W., Rix, H.-W., et al. 2016, *ApJ*, 823, 114
- Nidever, D. L., Bovy, J., Bird, J. C., et al. 2014, *ApJ*, 796, 38
- Nidever, D. L., Holtzman, J. A., Allende Prieto, C., et al. 2015, *AJ*, 150, 173
- Nissen, P. E. 2015, *A&A*, 579, A52
- Nissen, P. E., Silva Aguirre, V., Christensen-Dalsgaard, J., et al. 2017, *A&A*, 608, A112
- Pickering, J. C. 1996, *ApJS*, 107, 811
- Pinsonneault, M. H., Elsworth, Y., Epstein, C., et al. 2014, *ApJS*, 215, 19
- Roškar, R., Debattista, V. P., Quinn, T. R., Stinson, G. S., & Wadsley, J. 2008, *ApJ*, 684, L79
- Salaris, M., Pietrinferni, A., Piersimoni, A. M., & Cassisi, S. 2015, *A&A*, 583, A87
- Schiavon, R. P., Zamora, O., Carrera, R., et al. 2017, *MNRAS*, 465, 501
- Schönrich, R., & Binney, J. 2009a, *MNRAS*, 396, 203
- . 2009b, *MNRAS*, 399, 1145
- Sellwood, J. A., & Binney, J. J. 2002, *MNRAS*, 336, 785
- Shetrone, M., Bizyaev, D., Lawler, J., et al. 2015, *ArXiv e-prints*, arXiv:1502.04080
- Shetrone, M., T. J., et al. in prep
- Sneden, C., Lucatello, S., Ram, R. S., Brooke, J. S. A., & Bernath, P. 2014, *ApJS*, 214, 26
- Spina, L., Meléndez, J., & Ramírez, I. 2016, *A&A*, 585, A152
- Stanghellini, L., & Haywood, M. 2018, *ArXiv e-prints*, arXiv:1806.02276
- Tayar, J., Somers, G., Pinsonneault, M. H., et al. 2017, *ApJ*, 840, 17
- Twarog, B. A. 1980, *ApJ*, 242, 242
- van Zee, L., Salzer, J. J., Haynes, M. P., O'Donoghue, A. A., & Balonek, T. J. 1998, *AJ*, 116, 2805
- Weinberg, D. H., Andrews, B. H., & Freudenberg, J. 2017, *ApJ*, 837, 183
- Zamora, O., García-Hernández, D. A., Allende Prieto, C., et al. 2015, *AJ*, 149, 181
- Zasowski, G., Johnson, J. A., Frinchaboy, P. M., et al. 2013, *AJ*, 146, 81
- Zasowski, G., Cohen, R. E., Chojnowski, S. D., et al. 2017, *AJ*, 154, 198